Supporting Information

DOI:

About the Selectivity and Reactivity of Active Nickel Electrodes in C-C Coupling Reactions

Sebastian B. Beil, Manuel Breiner, Lara Schulz, Aaron Schüll, Timo Müller, Dieter Schollmeyer, Alexander Bomm, Michael Holtkamp, Uwe Karst, Wolfgang Schade, and Siegfried R. Waldvogel*

Table of Contents

1. General Remarks

All reagents were purchased from commercial suppliers or synthesized following the given literature protocols. No further purification was required. For standard electrolysis conditions 1,1,1,3,3,3-hexafluoroisopropanol (Fluorochem) and tetrabutylammonium hexafluorophosphate (ABCR, 98%) were used as received.

NMR spectroscopy: For measurements concerning NMR spectroscopy a multi-nuclear magnetic resonance spectrometer of the type AV II 400 (*Bruker,* analytic measuring technique, Karlsruhe, Germany) was employed. The chemical shifts were referenced on δ-value in ppm of the residue signal of the deuterated solvent ($CDCl_3$: ^1H = 7.26 ppm, ^{13}C = 77.2 ppm; C_6D_6: ^1H = 7.16 ppm, ^{13}C = 128.06 ppm; CD_2Cl_2: ^1H = 5.32 ppm, ^{13}C = 53.84 ppm; DMSO-d_6: ^1H = 2.50 ppm, ^{13}C = 39.52 ppm). ^{19}F signals were referenced to $CFCl_3$.

Gas chromatography: Reaction mixtures and purified products were analyzed *via* gas chromatography, for which a GC-2010 (*Shimadzu,* Japan) was used. The column is a quartz capillary column ZB-5 (length: 30 m, inner diameter: 0.25 mm, layer thickness of the stationary phase: 0.25 µm, carrier gas: hydrogen, stationary phase: (5%-phenyl)-polymethylsiloxane, *Phenomenex,* USA). The injector temperature was 250 °C with a linear carrier gas rate of 45.5 $cm \cdot s^{-1}$. Further gas chromatographic-mass spectra (GC-MS) were taken, using a GC-2010 combined with a mass detector GCMS-QP2010 (*Shimadzu,* Japan). It has a similar quartz capillary column ZB-5 (length: 30 m, inner diameter: 0.25 mm, layer thickness of the stationary phase: 0.25 µm, carrier gas: hydrogen, stationary phase: (5%-phenyl-methlpolysiloxane, *Phenomenex,* USA), whereas the ion source has a temperature of 200 °C. Four different methods were used for the GC-spectra measurements: method "*hart"* (starting temperature: 50 °C, heating rate: 15 °C/min, end temperature: 290 °C for 8 min), method "*hart 16 min"*, which is identical, but leaving out the last 8 minutes. Method "method1langextrahart" (starting temperature: 100 °C, heating rate: 15 °C/min, end temperature: 310 °C for 22 min) and method "method1" (starting temperature: 50 °C, heating rate: 10 °C/min, end temperature: 250 °C for 15 min) were also used.

Mass spectrometry: For high resolution electrospray ionization or atmospheric pressure chemical ionization mass spectrometry measurements, an Agilent 6545 Q-ToF MS was utilized. The field desorption mass spectra (FD) were accomplished with MAT 95 (*Thermo Finnigan*, Bremen).

IR spectroscopy: For IR measurements, a "Bruker Alpha II FTIR" spectrometer (*Bruker Corporation,* Massachusetts, USA) with a Platinum-ATR unit was used.

Melting points: The melting ranges were measured with "Melting Point Apparatus M-565" (*Büchi,* Essen, Germany). Heating rates of 5 °C min^{-1} were applied.

Preparative chromatography: For standard liquid chromatography separation silica gel 60 M (0.040-0.063 mm *Macherey-Nagel GmbH & Co.*, Düren, Germany) was used. An automatic silica flash column chromatography system was employed, which consists of a control unit C-620, a fraction collector C-660 and a UV photometer C-635 (*Büchi*, Flawil, Switzerland).
Thin-layer-chromatography was performed using "DC Kieselgel 60 F254" (*Merck KGaA,* Darmstadt, Germany) on aluminum and a UV lamp (*Benda*, NU-4 KL, λ = 254 nm, Wiesloch, Germany). The resulting retention factors (R*f*) are given in relation to the solvent ratio.

Software: Text was generated with Microsoft Office 2010. Figures and schemes were obtained from ChemDraw 12.0.2. NMR spectra were processed using MestReNova 12.0.0.

2. Electrochemical Setup

Galvanostat: For the electrolysis, a self-built eight-channel galvanostat with an integrated coulomb counter of the University Bonn was used.[1] For screening and small scale reactions 5 mL undivided Teflon cells were used (Scheme 1). These can be home-made according to the previous report[1] or the whole system can be purchased as IKA Screening System from IKA-Werke GmbH & Co KG, Staufen, Germany. For reactions on larger scale, 25 mL beaker-type cells were utilized (Scheme 2).

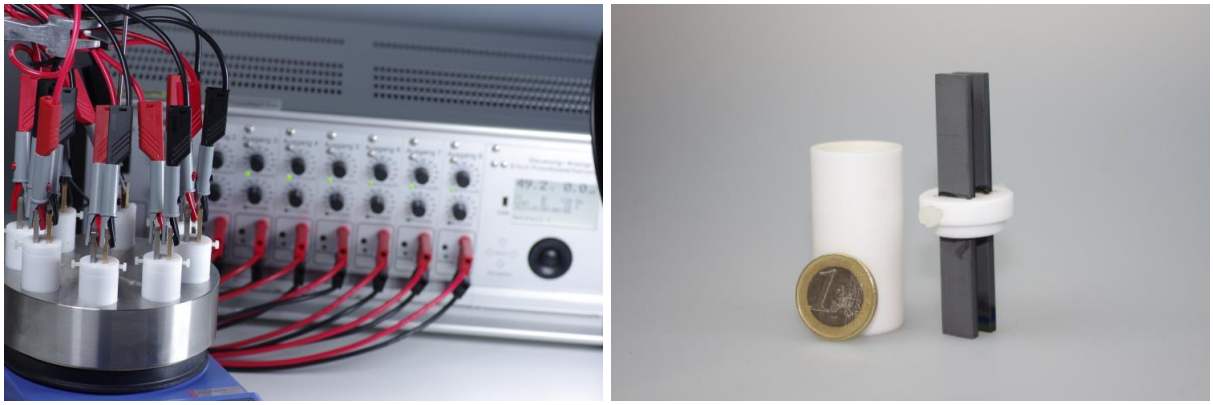

Figure S1: Design of the screening array with eight-channel galvanostatic device (left), 5 mL Teflon cell with two parallel electrodes; size of electrodes: 3 mm x 10 mm x 70 mm (right, not the final electrode material shown).

Figure S2: 25 mL beaker-type electrolysis cell; size of electrodes: 3 mm x 20 mm x 60 mm (not the final electrode materials shown).

Applied electrodes were cut mechanically into the respective size for screening or beaker-type electrolysis cells, with the respective thickness of the metals (Ni: 3 mm).

3. Electrode Screening

The following materials were applied as anodes:

Material	Supplier	Purity (%)
Molybdenum	Haines & Maassen Metallhandelsgesellschaft mbH Pützchens Chaussee 60 53227 Bonn, Germany	99.9
Nickel	IKA Werke GmbH & Co. KG Janke und Kunkel-Straße 10 79219 Staufen im Breisgau, Germany	99.5
Waspalloy®	Goodfellow GmbH Alstertwiete 3 20099 Hamburg, Germany GOODFELLOW (NI150450)	Ni 59, Cr 19.5, Co 13.5, Mo 4.2, Ti 3, Al 1.2, Fe <2, Mn 0.7, C 0.07
Ni/Cr	GOODFELLOW (NI053250)	Ni 75, Cr 19, Fe 5, Cu 0.5, Si 0.5, Ti 0.4
Inconel 625®	GOODFELLOW (NI040240)	Ni 61, Cr 21.5, Mo 9, Fe <5, Nb+Ta 3.65, Si<0.5, Al 0.25, Mn 0.25, Ti 0.25, C <0.1, S <0.015
Hastelloy C276®	GOODFELLOW (NI140550)	Ni 57, Mo 16-18, Cr 13-17.5, Fe 4.5-7, W 3.7-5.3, C <0.15
Monel® K-500	GOODFELLOW (NE043050)	Ni 63, Cu 30, AL 3, Fe 2, Mn 1.5, Ti 0.5

We tested Waspalloy, Ni/Cr, and Inconel as alloys, but surprisingly all resulted in lower product formation compared to neat nickel. All these three alloys exhibit a high content in chromium. However, pure chromium as anode was previously identified for successful dehydrogenative coupling but going along with significant corrosion.[2] Nevertheless, the combination of high nickel and chromium compositions gave diminished conversions (Table S1, Entries 2-4). A similar low yield of 24% for **2a** was observed when using Hastelloy, which consists mainly of nickel and molybdenum (Table S1, Entry 5). Hence, both metals are applicable in this homo-coupling reaction individually, the combination appears to be less favored. A reversed picture was obtained for Monel alloy, which provides a surprisingly high yield (Table S1, Entry 6). Due to the high copper content a low yield was anticipated, as noticed earlier where no reaction took place at a pure copper anode. Earlier, laser grafting (see Section 5) resulted in an improved yield for the active molybdenum anode, but did not work for nickel. Even a slightly lower yield was observed by GC analysis (Table S1, Entry 7).

Table S1: Various nickel alloys and geometries in the dehydrogenative coupling reaction of 4-fluoroveratrole (**1a**).

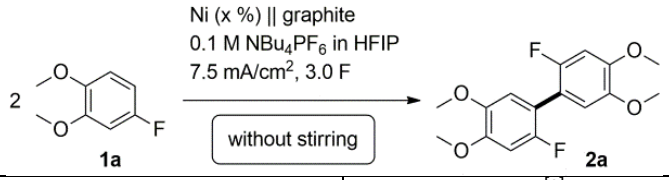

Entry	Anode	Ni content (%)[a]	Yield[b]
1	nickel	99.5	55
2	Waspalloy®	59	31
3	Ni/Cr	75	30
4	Inconel 625®	61	21
5	Hastelloy C276®	57	24
6	Monel® K-500	63	43
7	nickel V8.1[c]	99.5	48

[a] Content of nickel in the anode material/alloy wt%. For details on the nickel composition and morphology see table above. [b] GC yield for **2a** by internal calibration (see SI, section 7). [c] Laser-grafted surface as shown in Figure **S5**.

To investigate the performance of the electrode surface we applied the same nickel electrode in many consecutive dehydrodimerization reactions of fluoro veratrole (Figure S3). During the first three runs, the GC yield was constant at around 55%. Afterwards, the yield eroded constantly down to 10% after nine cycles. A plausible rationale is an in-situ formation of an electro-active layer.

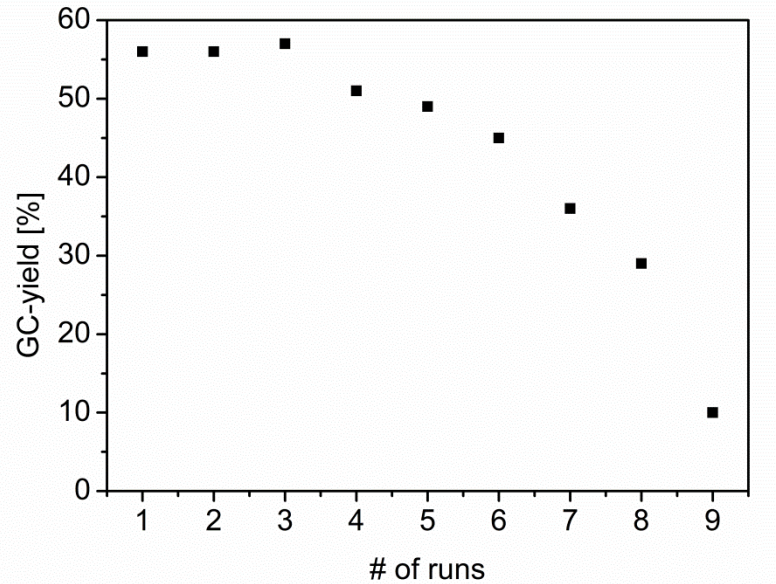

Figure S3: Long-term deactivation effect of a nickel anode in HFIP. GC yield of **2a** obtained with internal calibration after each electrolysis (see Section 7 and 8).

4. ICP-OES (inductively coupled plasma with optical emission spectrometry)

Instrument: ArCos MVII (Spectro GmbH, Kleve, Germany), radial view mode.
Plasma conditions: RF-Power: 1200 W; cooling gas (Ar): 13 L/min; aux gas (Ar): 0,8 L/min; nebulizer gas (Ar): 0,8 L/min.
Wavelength: Ni (232,003 nm, 221,648 nm, 231,604 nm) and Rh (IS) (343,489 nm).
Single element standards (Ni and Rh) were purchased from SCP-Science (Clark Graham Baie D'Urfé, Quebec, Canada).

GC-solutions of the respective samples showed distinct color depending on the substrate and whether stirring was applied.

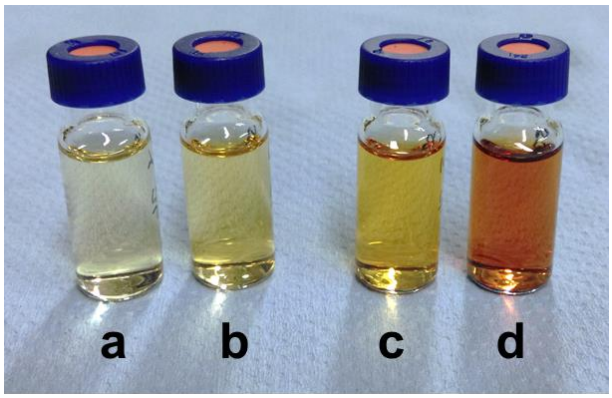

Figure S4: GC solution of samples (0.1 mL was diluted with ethyl acetate and filtered over silica for GC analysis). a) **1b** with stirring, b) **1b** without stirring, c) **1a** with stirring, d) **1a** without stirring.

In contrast, by GC analysis almost full conversion was found for **2b** either with or without stirring of the reaction mixture (Table S2, Entries 1 and 2). Surprisingly, product **2b** contained the twofold traces of nickel without stirring. When substrates with a low oxidation potential are applied (*e.g.* **1b**) the product formation is fast at the active electrode surface and after consumption of substrate, the nickel surface seems to dissolve without stirring. For halogenated substrates with a higher oxidation potential (e.g. **1a**) the product formation is promoted without stirring. The substrate dependence could also been visually followed by the respective GC solutions (Figure S4).

Table S2: Determination of nickel content upon electrolysis by ICP-OES.

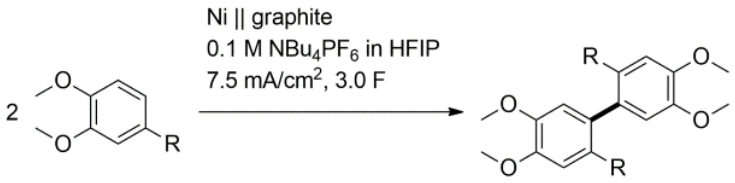

1a or **1b** **2a** or **2b**

Entry	R	Substrate [GC/%]	Product [GC/%]	Stirring	Ni content [ppm]
1	Me	4	93	yes	43.0±4.9
2	Me	2	96	no	89.9±6.1
3	F	77	19	yes	59.9±1.8
4	F	26	62	no	57.1±5.2

5. Laser-Grafted Nickel Surfaces

Nickel plates with a thickness of 3.0 mm have been cleaned by ultrasonication with acetone and deionized water. For laser microstructuring, an *AMPHOS* 400 Yb:YAG high power laser system at a centre wavelength of λ = 1030 nm has been applied. By a grating compressor, the final pulse length of τ = 0.75 ps has been achieved. A spot diameter of approximately 94 µm ($1/e^2$) after a 420 mm f-theta objective has been used. The average output power of P = 23.7 W in combination with the repetition rate of f = 1 MHz results in a pulse energy of E = 23.7 µJ and a performance of J = 0.34 Jcm^{-2} per shot. The samples have been processed with a continuous speed of v = 0.05 ms^{-1}. Each spot on the surface has been hit N = 1879 times by the laser beam. Areas of 70 mm x 10 mm have been irradiated with a meandering pattern scan in lines with a distance of D = 5 µm. The chamber has been flooded by a constant flow with argon of about v = 12 ms^{-1} to provide a clean surface area.

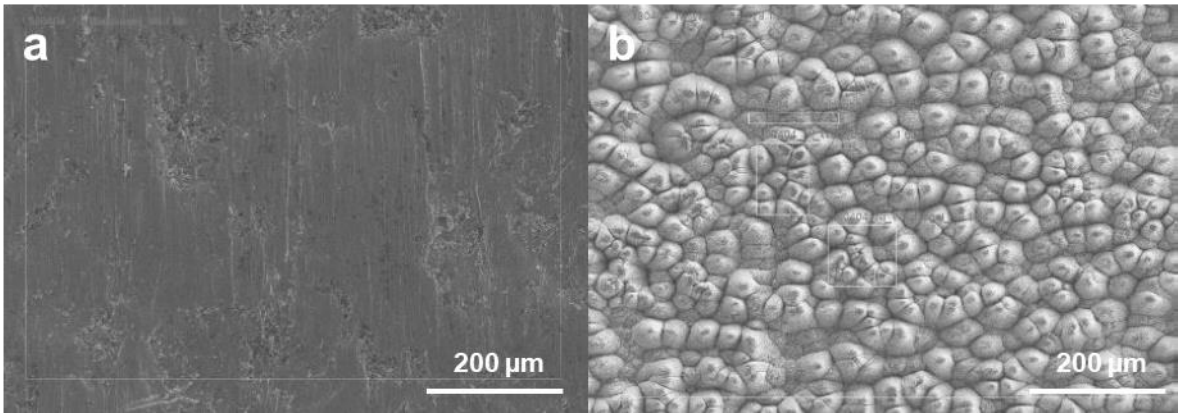

Figure S5: REM images of (a) planar and (b) micro-structured nickel electrodes (nickel V8.1).

6. GC Calibration with Internal Standard

6.1. GC Calibration Curve

The indicated amount 2,2'-difluor-4,4',5,5'-tetramethoxy-1,1'-biphenyl (t_R(GC 3, "hart")=14.35 min) and 30 mg (0.12 mmol) 3,3',5,5'-tetramethyl-2,2'-biphenol (t_R(GC 3, "hart")=12.67 min) as standard are dissolved in 5 mL of an 0.1 M NBu_4PF_6 solution in HFIP. 0.5 mL of this solution is filtered through silica gel (1.5 g, silica gel 60) with 2.5 mL ethyl acetate and analyzed *via* gas chromatography. The quotients were calculated from the weight of the biphenyl m_p and the biphenol m_s, as well as from the GC integrals P_p and P_s. With this data, the calibration graph was set up.

Table S3: Masses $\boldsymbol{m_p}$ of the product and $\boldsymbol{m_S}$ of the standard as well as quotient $\frac{\boldsymbol{m_P}}{\boldsymbol{m_S}}$ with respective errors.

Entry	$\boldsymbol{m_P}$/mg	$\Delta\boldsymbol{m_P}$/mg	$\boldsymbol{m_S}$/mg	$\Delta\boldsymbol{m_S}$/mg	$\frac{\boldsymbol{m_P}}{\boldsymbol{m_S}}$	$\Delta\frac{\boldsymbol{m_P}}{\boldsymbol{m_S}}$
1	10	±1	30	±1	0.33	±0.03
2	20	±1	30	±1	0.67	±0.04
3	30	±1	30	±1	1.00	±0.05
4	40	±1	30	±1	1.33	±0.06
5	50	±1	30	±1	1.67	±0.06
6	65	±1	30	±1	2.17	±0.08
7	80	±1	30	±1	2.67	±0.09

The error from the analytical balance was used as mass errors. The error of the quotient was calculated by the propagation of errors:

$$\Delta\frac{m_P}{m_S} = \sqrt{\left(\frac{\Delta m_P}{m_S}\right)^2 + \left(\frac{\Delta m_S m_P}{m_S^2}\right)^2} \quad (1)$$

Table S4: GC-Integrals $\boldsymbol{P_p}$ of the product and $\boldsymbol{P_S}$ of the standard as well as quotient $\frac{\boldsymbol{P_P}}{\boldsymbol{P_S}}$ with respective errors.

Entry	$\boldsymbol{P_P}$	$\Delta\boldsymbol{P_P}$	$\boldsymbol{P_S}$	$\Delta\boldsymbol{P_S}$	$\frac{\boldsymbol{P_P}}{\boldsymbol{P_S}}$	$\Delta\frac{\boldsymbol{P_P}}{\boldsymbol{P_S}}$
1	13377	±1149	60532	±391	0.22	±0.02
2	20688	±1149	52429	±391	0.39	±0.02
3	27806	±1149	42627	±391	0.65	±0.03
4	46601	±1149	51288	±391	0.91	±0.02
5	67890	±1149	54730	±391	1.24	±0.02
6	108520	±1149	66270	±391	1.64	±0.02
7	123172	±1149	58682	±391	2.10	±0.02

The integral errors were obtained by measuring the sample **3** three times in a row and calculating the average value and the standard error:

Table S5: Values for the calculation of the Integral errors.

	P_P	P_S
Measurement 1	27806	42627
Measurement 2	26116	42786
Measurement 3	25612	42043
Average $\bar{P}$	26511	42485
Standard error ΔP	$\pm$1149	$\pm$391

$$\bar{P} = \frac{1}{n}\sum_{i=1}^{n} P_i \tag{2}$$

$$\Delta P = \frac{1}{\sqrt{n}}\sqrt{\frac{\sum_{i=1}^{n}(P_i - \bar{P})^2}{n-1}} \tag{3}$$

The error of the quotient was again calculated by the propagation of errors:

$$\Delta\frac{P_P}{P_S} = \sqrt{\left(\frac{\Delta P_P}{P_S}\right)^2 + \left(\frac{\Delta P_S P_P}{P_S^2}\right)^2} \tag{4}$$

The calibration graph was created using the data in table 6.2 and 6.3:

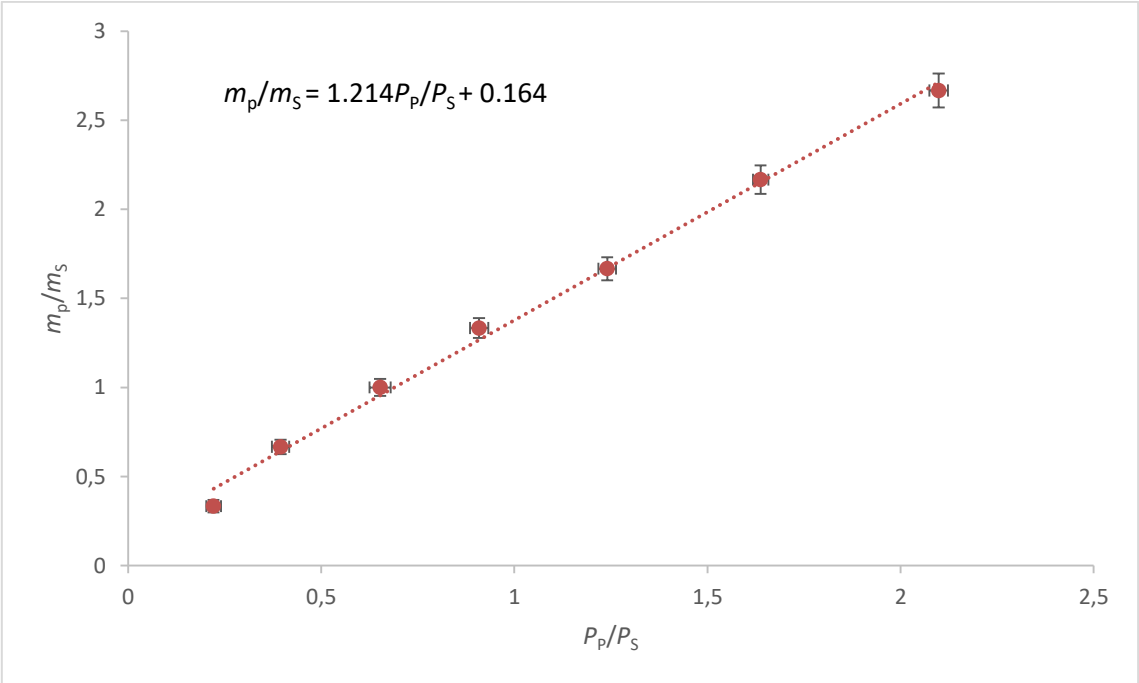

Figure S6: Calibration line for the internal calibration.

6.2. Analysis of the Electrolysis Mixture

After the electrolysis was finished, 30 mg (0.12 mmol) 3,3',5,5'-tetramethyl-2,2'-biphenol was added to the reaction mixture while stirring. 0.5 mL of this mixture was taken from the cell and filtered through silica gel (1.5 g, silica gel 60) and rinsed with 2.5 mL ethyl acetate. The filtrate was analyzed by GC. With the aid of the calibration line, the mass of the product could then be calculated:

$$m_{\mathrm{P}}^{\mathrm{GC}} = 30\ \mathrm{mg} \cdot \left[1.214 \cdot \frac{P_{\mathrm{P}}}{P_{\mathrm{S}}} + 0.164\right] \tag{4}$$

The corresponding error $\Delta m_{\mathrm{P}}^{\mathrm{GC}}$ was calculated by:

$$\Delta m_{\mathrm{P}}^{\mathrm{GC}} = \sqrt{\left[\Delta m_{\mathrm{S}} \cdot \left(1.214 \cdot \frac{P_{\mathrm{P}}}{P_{\mathrm{S}}} + 0.164\right)\right]^2 + \left[1.214 \cdot \Delta\frac{P_{\mathrm{P}}}{P_{\mathrm{S}}} \cdot m_{\mathrm{s}}\right]^2} \tag{5}$$

The GC yield was then calculated using the weighed in mass of the starting material m_{SM}, the molar mass of the starting material $M_{\mathrm{SM}} = 156.15\frac{\mathrm{g}}{\mathrm{mol}}$ and the molar mass of the product $M_{\mathrm{P}} = 310.29\frac{\mathrm{g}}{\mathrm{mol}}$ with equation 6:

$$\mathrm{Yield}_{\mathrm{GC}} = \frac{\frac{m_{\mathrm{P}}^{\mathrm{GC}}}{M_{\mathrm{p}}}}{0.5 \cdot \frac{m_{\mathrm{SM}}}{M_{\mathrm{SM}}}} \cdot 100\% \tag{6}$$

The corresponding error was calculated using equation 7, the error of the weighed in starting material was set to $\Delta m_{\mathrm{SM}} = \pm 5\ \mathrm{mg}$. In this case, the error is larger than the scale error, as exact the dosing of the liquid starting material is rather difficult.

$$\Delta\mathrm{Yield}_{\mathrm{GC}} = \sqrt{\left(\frac{M_{\mathrm{SM}}\Delta m_{\mathrm{P}}^{\mathrm{GC}}}{m_{\mathrm{SM}}M_{\mathrm{P}}}\right)^2 + \left(\frac{m_{\mathrm{P}}^{\mathrm{GC}}M_{\mathrm{P}}\Delta m_{\mathrm{SM}}}{m_{\mathrm{SM}}^2 M_{\mathrm{P}}}\right)^2} \cdot 100\% \tag{7}$$

With this method, only the ratio between formed product and internal standard is taken into account. The occurrence of possible side products during the electrolysis can be neglected, making the results more reliable.

7. Reaction Optimization

General protocol for reaction optimization

156 mg (1 mmol) 1,2-dimethoxy-4-fluorobenzene and the corresponding supporting electrolyte (0.1 M) were dissolved in 5 mL HFIP (+additive) in an undivided screening-cell and electrolyzed. After the electrolysis, the reaction mixture was analyzed *via* internal calibration. The individual reaction parameters are listed in the corresponding tables below. As the initial optimization steps with stirring lead to significantly lower yields in all cases, only the optimization without stirring is shown.

Whenever pure Nickel was used as anode material, the electrodes were polished directly before use with fine sandpaper (P400 and P1000) and rinsed with acetone.

Optimization of the current density

Table S6: Optimization of current density. Reaction conditions: Ni anode, graphite cathode, RT, 3 F, 0.1 M NBu_4PF_6, reaction carried out without stirring.

Entry	Current density/$\frac{mA}{cm^2}$	GC yield/%
1	4	41±1
2	5	47±1
3	6	48±1
4	7	47±1
5	7.5	48±1
6	8	48±1
7	9	45±1
8	10	44±1

Optimization of the supporting electrolyte

Table S7: Optimization of supporting electrolyte (0.1 M). Reaction conditions: Ni anode, graphite cathode, RT, 3 F, 7.5 mA/cm^2, reaction carried out without stirring.

Entry	Supporting electrolyte	GC yield/%
1	NBu_4PF_6	53±2
2	NBu_4BF_4	49±1
3	NBu_4Br	0
4	NBu_4I	0
5	NBu_4Cl	0
6	NBu_4HSO_4	6±1
7	NBu_4ClO_4	20±1
8	NBu_4Br_3	0

Optimization of the applied charge

Table S8: Optimization of applied charge**.** Reaction conditions: Ni anode, graphite cathode, RT, 7.5 mA/cm^2, 0.1 M NBu_4PF_6, reaction carried out without stirring.

Entry	Applied charge/F	GC yield/%
1	1.5	42±1
2	2	45±1
3	2.5	48±2
4	3	46±1
5	3.5	46±1
6	4	43±1
7	4.5	34±1
8	5	30±1

Optimization of the substrate concentration

Table S9: Optimization of concentration**.** Reaction conditions: Ni anode, graphite cathode, RT, 7.5 mA/cm^2, 0.1 M NBu_4PF_6, 3.0 F, reaction carried out without stirring.

Entry	Substrate concentration/$\frac{mol}{L}$	GC yield/%
1	0.05	34±1
2	0.1	48±2
3	0.15	45±1
4	0.2	53±2
5	0.3	57±2
6	0.4	50±2

Entry 5 and 6 showed overoxidation products as well as unconverted substrate, providing double negative properties.

Optimization of the anode material

Table S10: Variation of the anode. Reaction conditions: graphite cathode, RT, 3 F, 0.1 M NBu_4PF_6, 7.5 mA/cm^2, reaction carried out without stirring.

Entry	Anode material	GC yield/%
1	Ni	47±1
2	Waspalloy	31±1
3	Ni/Cr	30±1
4	Inconel	21±1
5	Hastelloy	24±1
6	Monel	43±1
7	nano V8	40±1
8	Nano V8.1	48±1

Optimization of the reaction temperature

Table S11: Variation of the temperature. Reaction conditions: Ni-anode, graphite cathode, 3 F, 0.1 M NBu_4PF_6, 7.5 mA/cm^2, reaction carried out without stirring.

Entry	Temperature/°C	GC yield/%
1	10	50±2
2	20	51±1
3	RT (≈25)	55±2
4	30	45±1
5	40	43±1
6	50	39±1

Long term stability test without electrode polishing

Table S12: Long term stability without pretreatment. Reaction conditions: Ni-anode, graphite cathode, 3 F, 0.1 M NBu_4PF_6, 7.5 mA/cm^2, reaction carried out without stirring.

Entry	Electrolysis	GC yield/%
1	1st	56±2
2	2nd	56±2
3	3rd	57±2
4	4th	51±2
5	5th	49±1
6	6th	45±1
7	7th	36±1
8	8th	29±1
9	9th	10±1

For all reactions, the same electrode was used without polishing between electrolysis.

8. CV measurements

Oxidation potentials of the applied arenes could not be determined using a nickel electrode tip due to the formation of the electroactive $Ni_x(HFIP)_y$ layer. Figure S7a shows the first three scans of the freshly polished nickel working electrode in the blank electrolyte system at a relatively low scan rate of 20 mV/s. Starting at approximately 1.25 V (vs. Ag/AgCl) an irreversible oxidative current occurs which peaks at 1.9 V (vs. Ag/AgCl) and then merges into the decomposition of the electrolyte. This peak is assigned to the formation of the active electrode layer. The lower currents in the following scans can be explained by the incomplete dissolution of this stable active layer during the reverse scan. This oxidation peak can only be observed at low scan rates and vanishes at 100 mV/s (Figure S8). Figure S7b exemplary shows the cyclic voltammograms of the electrolyte (black curve), the electrolyte with the substrate (blue curve) and the electrolyte with ferrocene (red curve) at low scan rates of 20 mV/s. Between each of these measurements, the working electrode was polished and the other electrodes were rinsed with ethanol to avoid contamination. Interestingly, the substrate shows now distinct oxidation peak, but a strong, linear oxidative current was observed above the potential of the electroactive layer formation (off-set at 1.25 V vs. Ag/AgCl). This indicates that the oxidation of the substrate is not converted directly at the nickel surface, but at the electrocatalytic layer which is then constantly regenerated. Transformation of the substrate could also be observed macroscopically as blue streaks formed at the working electrode at potentials above 1.25 V vs Ag/AgCl (compare Figure S7 c and d). Also ferrocene did not show a reversible redox behavior, no oxidative current could be observed at all, showing the unusual behavior and high selectivity of the electroactive layer.

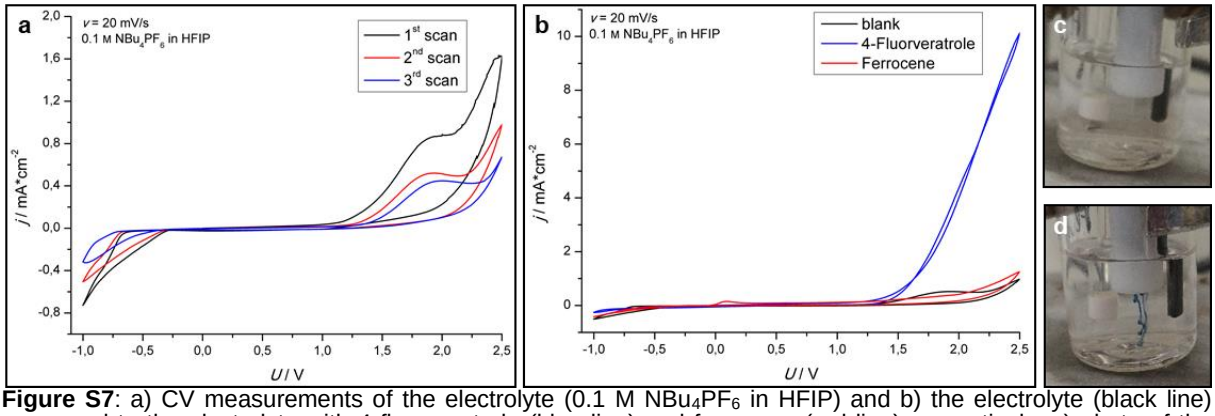

Figure S7: a) CV measurements of the electrolyte (0.1 M NBu_4PF_6 in HFIP) and b) the electrolyte (black line) compared to the electrolyte with 4-fluorveratrole (blue line) and ferrocene (red line) respectively. c) photo of the electrolyte containing 4-Fluorveratrole before and d) after passing the potential of 1.25 V vs Ag/AgCl. WE: Nickel electrode tip, 2 mm diameter; CE: glassy carbon rod; RE: Ag/AgCl in saturated LiCl/EtOH.

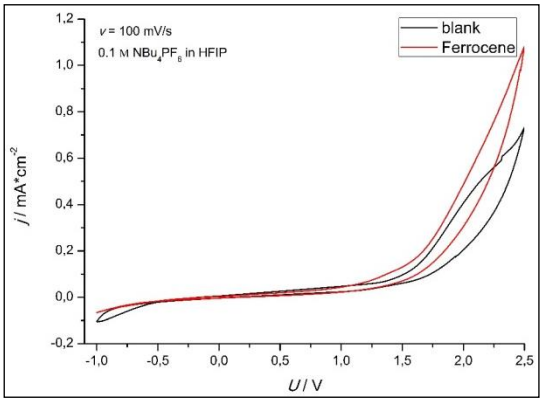

Figure S8: CV measurement of the electrolyte (0.1 M NBu_4PF_6 in HFIP; black line) and Ferrocene in the respective electrolyte (red line). WE: nickel electrode tip, 2 mm diameter; CE: glassy carbon rod; RE: Ag/AgCl in saturated LiCl/EtOH.

9. Synthesis

General Protocol for Electrolysis

For each reaction the substrate and tetrabutylammonium hexafluorophosphate (0.5 mmol, 194 mg) were dissolved in HFIP (5.0 mL) in an undivided electrolysis cell equipped with a nickel anode[1] and graphite cathode. The electrodes were immersed in the solution and the applied charge was set to 1.5 F referring to **2**. The current density was 7.5 mA/cm². While the reaction was in progress the solution was stirred or not stirred. The reaction mixture was purified by silica flash column chromatography using cyclohexane and EtOAc. For analytical purpose the isolated products were further recrystallized from methanol.

2,2'-Dibromo-5,5'-difluoro-4,4'-dimethoxy-1,1'-biphenyl (2c)

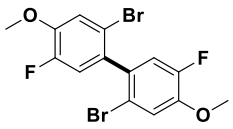

5-Bromo-2-fluoroanisole (201 mg, 1.0 mmol) was treated with 145 C (1.5 F) without stirring. The reaction mixture was purified by silica flash column chromatography (1% → 5% EtOAc in cyclohexane) to obtain the product as colorless needles (140 mg, 0.34 mmol, 69%).
^{1}H NMR (400 MHz, $CDCl_3$): δ = 7.22 (d, $^4J_{HF}$ = 8.0 Hz, 2H), 6.98 (d, $^3J_{HF}$ = 11.3 Hz, 2H), 3.93 (s, 6H) ppm. **GCMS:** 13.9 min (method "hart"), *m/z* = 406 (51), 408 (100), 410 (49).
Analytical data are in agreement with previous results.[2]

2,2'-Dibromo-5,5'-dichloro-4,4'-dimethoxy-1,1'-biphenyl (2d)

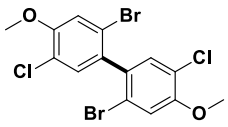

5-Bromo-2-chloroanisole (230 mg, 1.0 mmol) was treated with 145 C (1.5 F) without stirring. The reaction mixture was purified by silica flash column chromatography (10% → 20% EtOAc in cyclohexane) to obtain the product as colorless needles (174 mg, 0.38 mmol, 76%).
^{1}H NMR (400 MHz, $CDCl_3$): δ = 7.23 (s, 2H), 7.19 (s, 2H), 3.95 (s, 6H) ppm. **GCMS:** 17.4 min (method "hart"), *m/z* = 441.
Analytical data are in agreement with previous results.[2]

2,2'-Dichloro-4,4'-dimethoxy-5,5'-dimethyl-1,1'-biphenyl (2e)

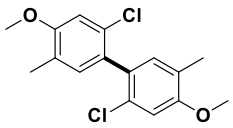

5-Chloro-2-methylanisole (156 mg, 1.0 mmol) was treated with 145 C (1.5 F) without stirring. The reaction mixture was purified by silica flash column chromatography (1% → 5% EtOAc in cyclohexane) to obtain the product as yellow needles (72 mg, 0.23 mmol, 47%).
^{1}H NMR (400 MHz, $CDCl_3$): δ = 7.01 (q, ^4J = 0.9 Hz, 2H), 6.91 (s, 2H), 3.93 (s, 6H), 2.20 (s, 6H) ppm. **^{13}C NMR** (101 MHz, $CDCl_3$): δ = 157.7, 133.2, 131.4, 130.0, 125.2, 111.0, 55.7, 15.9 ppm. **HR-MS** (APCI): *m/z* calculated for $C_{16}H_{16}Cl_2O_2$ $[M+H]^+$: 310.0527, found: 310.0525. **GC:** 14.280 min (method "hart"). **GCMS:** 15.2 min (method "hart"), *m/z* = 310 (100), 312 (65), 314 (11). **Mp:** 136.7-138.9 °C. **R_f:** 0.50 (cyclohexane:EtOAc, 99:1).

2,2'-Dibromo-4,4'-dimethoxy-5,5'-dimethyl-1,1'-biphenyl (2f)

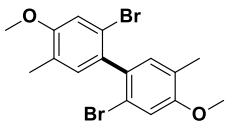

5-Bromo-2-methylanisole (208 mg, 1.0 mmol) was treated with 145 C (1.5 F) without stirring. The reaction mixture was purified by silica flash column chromatography (10% → 15% EtOAc in cyclohexane) to obtain the product as colorless needles (92 mg, 0.22 mmol, 44%).
^{1}H NMR (400 MHz, $CDCl_3$): δ = 7.07 (s, 2H), 6.99 (s, 2H), 3.86 (s, 6H), 2.18 (s, 6H) ppm. **GCMS:** 15.9 min (method "hart"), *m/z* = 400.
Analytical data are in agreement with previous results.[2]

[1] After each run the anode was polished with fine sand paper (P400) and rinsed with acetone.

4,4'-Dimethoxy-2,2',6,6'-tetramethyl-1,1'-biphenyl (2g)

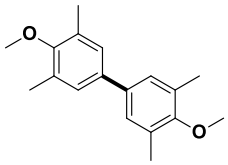

2,6-Dimethylanisole (140 mg, 1.0 mmol) was treated with 145 C (1.5 F) without stirring. The reaction mixture was purified by silica flash column chromatography (10% → 30% EtOAc in cyclohexane) to obtain the product as yellow oil (43 mg, 0.16 mmol, 31%).
^{1}H NMR (400 MHz, $CDCl_3$): δ = 7.20 (s, 4H), 3.76 (s, 6H), 2.35 (s, 12H) ppm. **GCMS:** 14.7 min (method "hart"), *m/z* = 270.
Analytical data are in agreement with previous results.[3]

2,2'-Difluoro-4,4',5,5'-tetramethoxy-1,1'-biphenyl (2a)

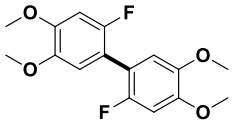

1,2-Dimethoxy-4-fluoro-benzene (156 mg, 1.0 mmol) was treated with 145 C (1.5 F) without stirring. The reaction mixture was purified by silica flash column chromatography (10% → 12% EtOAc in cyclohexane) to obtain the product as colorless needles (65 mg, 0.21 mmol, 42%).
^{1}H NMR (400 MHz, $CDCl_3$): δ = 6.85 (m, 2H), 6.73 (m, 2H), 3.90 (s, 6H), 3.88 (s, 6H) ppm. **GCMS:** 14.3 min (method "hart"), *m/z* = 310.
Analytical data are in agreement with previous results.[2]

2,2'-Dibromo-4,4',5,5'-tetramethoxy-1,1'-biphenyl (2b)

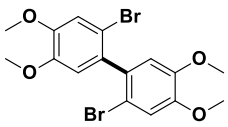

4-Bromo-1,2-dimethoxy-benzene (230 mg, 1.0 mmol) was treated with 145 C (1.5 F) with and without stirring. The reaction mixture was purified by silica flash column chromatography (10% → 30% EtOAc in cyclohexane) to obtain the product as colorless needles (with stirring: 114 mg, 0.25 mmol, 50%; without stirring: 168 mg, 0.38 mmol, 76%).
^{1}H NMR (400 MHz, $CDCl_3$): δ = 7.11 (s, 2H), 6.76 (s, 2H), 3.92 (s, 6H), 3.86 (s, 6H) ppm. **GCMS:** 17.3 min (method "hart"), *m/z* = 432.
Analytical data are in agreement with previous results.[2]

4,4',5,5'-Tetramethoxy-2,2'-dimethyl-1,1'-biphenyl (2h)

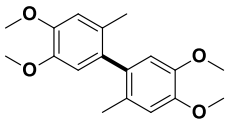

1,2-Dimethoxy-4-methyl-benzene (151 mg, 1.0 mmol) was treated with 145 C (1.5 F) with and without stirring. The reaction mixture was purified by silica flash column chromatography (10% → 30% EtOAc in cyclohexane) to obtain the product as colorless needles (with stirring: 79 mg, 0.26 mmol, 52%; without stirring: 111 mg, 0.35 mmol, 69%).
^{1}H NMR (400 MHz, $CDCl_3$): δ = 6.77 (s, 2H), 6.65 (s, 2H), 3.91 (s, 6H), 3.83 (s, 6H), 2.02 (s, 6H) ppm. **GCMS:** 15.1 min (method "hart"), *m/z* = 302.
Analytical data are in agreement with previous results.[2]

2,2',4,4',5,5'-Hexamethoxy-1,1'-biphenyl (2i)

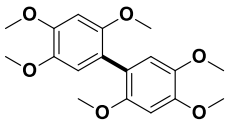

1,2,4-Trimethoxybenzene (178 mg, 1.0 mmol) was treated with 145 C (1.5 F) with and without stirring. The reaction mixture was purified by silica flash column chromatography (10% → 30% EtOAc in cyclohexane) to obtain the product as colorless needles (with stirring: 106 mg, 0.30 mmol, 60%; without stirring: 86 mg, 0.25 mmol, 50%).
^{1}H NMR (400 MHz, $CDCl_3$): δ = 6.82 (s, 2H), 6.63 (s, 2H), 3.93 (s, 6H), 3.84 (s, 6H), 3.76 (s, 6H) ppm. **GCMS:** 16.7 min (method "hart"), *m/z* = 334.
Analytical data are in agreement with previous results.[2]

2,2'-Di(ethoxycarbonylmethyloxy)-4,4'-dimethoxy-6,6'-dimethyl-biphenyl (2j)

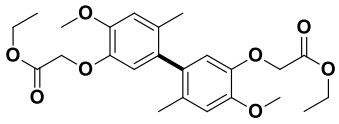

Ethyl 2-(2-methoxy-4-methylphenoxy)acetate (224 mg, 1.0 mmol) was treated with 145 C (1.5 F) without stirring. The reaction mixture was purified by silica flash column chromatography (10% → 20% EtOAc in cyclohexane) to obtain the product as colorless needles (125 mg, 0.28 mmol, 56%).

^{1}H NMR (400 MHz, $CDCl_3$): δ = 6.77 (s, 2H), 6.56 (s, 2H), 4.63 (d, 4H), 4.22 (q, ^{3}J = 8.0 Hz, 4H), 3.90 (s, 6H), 1.98 (s, 6H), 1.25 (t,^{3}J = 8.0 Hz, 6H) ppm. **^{13}C NMR** (101 MHz, $CDCl_3$): δ = 169.1, 148.4, 144.7, 132.9, 130.1, 115.9, 113.6, 66.7, 61.2, 56.0, 19.4, 14.2 ppm. **HR-MS** (ESI): *m/z* calculated for $C_{24}H_{30}O_8Na$ $[M+Na]^+$: 469.1838, found: 469.1841. **GC:** 17.74 min (method "hart"). **GCMS:** 20.7 min (method "hart"), *m/z* = 446. **Mp:** 62–64 °C. **R_f:** 0.33 (cyclohexane:EtOAc, 7:3).

5,5'-Dibromo-2,2',4,4'-tetramethoxy-biphenyl (2ka) and 1,5-Dibromo-2,4-dimethoxy-benzene (2kb)

1-Bromo-2,4-dimethoxy-benzene (228 mg, 1.0 mmol) was treated with 145 C (1.5 F) without stirring. The reaction mixture was purified by silica flash column chromatography (10% → 30% EtOAc in cyclohexane) to obtain the coupling product as colorless needles (24 mg, 0.06 mmol, 11%).

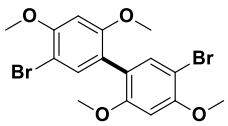

^{1}H NMR (400 MHz, $CDCl_3$): δ = 7.35 (s, 2H), 6.55 (s, 2H), 3.94(s, 6H), 3.79 (s, 6H) ppm. **GC:** 17.38 min (method "hart"). **GCMS:** 18.4 min (method "hart"), *m/z* = 430 (52), 432 (100), 434 (52);

and the bromination product as colorless needles (70 mg, 0.16 mmol, 31%). **^{1}H NMR** (400 MHz, $CDCl_3$): δ = 3.90 (s, 6H), 6.49 (s, 1H), 7.66 (s, 1H) ppm. **GCMS:** 11.7 min (method "hart"), *m/z* = 294 (50), 296 (100), 298 (50).

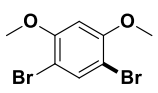

Analytical data are in agreement with previous results.[4]

3-(Cyano-(3,4-dimethoxyphenyl)methyl)-4-cyanomethyl-1,2-dimethoxybenzene (2l)

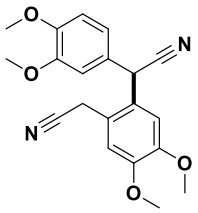

3,4-Dimethoxyphenyl acetonitrile (887 mg, 5.0 mmol) in 25 mL HFIP was treated with 725 C (1.5 F) without stirring. The reaction mixture was purified by silica flash column chromatography (10% → 30% EtOAc in cyclohexane) to obtain the product as colorless needles (456 mg, 1.3 mmol, 51%).

^{1}H NMR (400 MHz, $CDCl_3$): δ = 6.96 (s, 1H), 6.94 (s, 1H), 6.82 (d, ^{3}J = 8.0 Hz. 1H), 6.76 (dd, ^{3}J = 8.0 Hz, ^{4}J = 4.0 Hz, 1H), 6.73 (d, ^{4}J = 4.0 Hz, 1H), 5.20 (s, 1H), 3.92 (s, 3H), 3.88 (s, 3H), 3.86 (s, 3H), 3.82 (s, 3H), 3.55 (q, ^{2}J = 16.0 Hz, 2H) ppm. **^{13}C NMR** (101 MHz, $CDCl_3$): δ = 149.8, 149.5, 149.4, 149.3, 126.2, 125.3, 120.4, 119.9, 119.1, 117.3, 112.9, 112.7, 111.6, 110.5, 56.3, 56.3, 56.1, 56.1, 39.2, 21.1 ppm. **HR-MS** (ESI): *m/z* calculated for $C_{20}H_{20}N_2O_4Na$ $[M+Na]^+$: 375.1321, found: 375.1321. **GC:** 16.63 min (method "hart"). **GCMS:** 19.0 min (method "hart"), *m/z* = 352. **Mp:** 145–146 °C. **R_f:** 0.15 (cyclohexane:EtOAc, 7:3).

4-(Cyano-(3,4-dimethyoxyphenyl)methyl)biphenyl (4a) and 4-(Cyano-(3,4-dimethyoxyphenyl)-(2',2',2'-trifluoroethyl-(1'-trifluoromethyl)oxy)-methyl)biphenyl (4a')

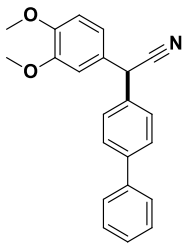

3,4-Dimethoxyphenyl acetonitrile (177 mg, 1.0 mmol) and biphenyl (308 mg, 2.0 mmol, 2.0 eq.) in 5 mL HFIP was treated with 288 C (3.0 F) with stirring. The reaction mixture was purified by silica flash column chromatography (17% → 25% EtOAc in cyclohexane) to obtain the product as orange solid (109 mg, 0.33 mmol, 33%).

^{1}H NMR (400 MHz, CD_3CN): δ = 7.68 – 7.59 (m, 4H), 7.51 – 7.42 (m, 4H), 7.39 – 7.34 (m, 1H), 6.99 – 6.91 (m, 3H), 5.35 (s, 1H), 3.78 (s, 6H) ppm. **^{13}C NMR** (101 MHz, CD_3CN): δ = 150.6, 150.1, 141.6, 140.9, 137.2, 129.9, 129.9, 128.9, 128.7, 128.6, 127.9, 121.1, 120.8, 113.0, 112.1, 56.5, 56.4, 42.0 ppm. **HR-MS** (APCI): *m/z* calculated for $C_{22}H_{19}NO_2$ $[M]^+$: 329.1416, found: 329.1402. **GC:** 18.17 min (method "hart"). **GCMS:** 20.00 min (method "hart"), *m/z* = 329. **R_f:** 0.17 (cyclohexane:EtOAc, 5:1).

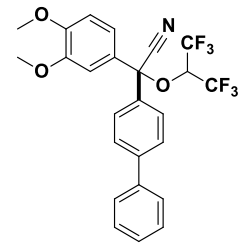

As byproduct a colorless oil was obtained (61 mg, 0,12 mmol, 12%).

^{1}H NMR (400 MHz, CD_3CN): δ = 7.75 (d, ^{3}J = 8.7 Hz, 2H), 7.69 – 7.65 (m, 2H), 7.59 (d, ^{3}J = 8.7 Hz, 2H), 7.50 – 7.44 (m, 2H), 7.43 – 7.37 (m, 1H), 7.18 (dd, $^{3,4}J$ = 8.5, 2.3 Hz, 1H), 7.02 (d, ^{3}J = 8.5 Hz, 1H), 6.94 (d, ^{4}J = 2.3 Hz, 1H), 5.00 (hept, $^{3}J_{HF}$ = 5.8 Hz, 1H), 3.84 (s, 3H), 3.73 (s, 3H) ppm. **^{13}C NMR** (101 MHz, CD_3CN): δ = 152.1, 150.5, 143.5, 140.4, 137.4, 130.0, 129.1, 128.5, 128.4, 128.0, 122.1, 118.2, 112.3, 111.8, 84.4, 72.3 (q, *J* = 32.9 Hz), 56.5, 56.4 ppm.[2] **^{19}F NMR** (376 MHz, CD_3CN): δ = -73.6 (qd, *J* = 9.8, 6.0 Hz), -73.9 (qd, *J* = 9.7, 5.6 Hz) ppm. **HR-MS** (APCI): *m/z* calculated for $C_{25}H_{19}F_6NO_3$ $[M]^+$: 495.1269, found: 495.1248. **GC:** 16.17 min (method "hart"). **GCMS:** 17.66 min (method "hart"), *m/z* = 495. **R_f:** 0.40 (cyclohexane:EtOAc, 5:1).

4-(Cyano-(5-dimethylethyl-2-methoxyphenyl)methyl)1,2-dimethoxybenzene (4b)

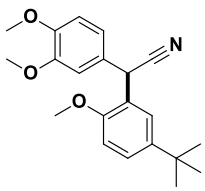

3,4-Dimethoxyphenyl acetonitrile (88.6 mg, 0.5 mmol) and 4-*tert*-butyl anisole (176 mg, 1.3 mmol, 2.6 eq.) in 5 mL HFIP was treated with 144.7 C (3.0 F) with stirring. The reaction mixture was purified by silica flash column chromatography (17% EtOAc in cyclohexane) and by reversed phase column chromatography (50% → 0% H_2O in MeCN) to obtain the product as orange oil (29 mg, 0.09 mmol, 17%).

^{1}H NMR (400 MHz, $CDCl_3$): δ = 7.35 (d, ^{4}J = 2.5 Hz, 1H), 7.31 (dd, $^{3,4}J$ = 8.6, 2.5 Hz, 1H), 6.93 – 6.88 (m, 2H), 6.83 (d, ^{3}J = 8.6 Hz, 1H), 6.82 (d, ^{3}J = 8.2 Hz, 1H), 5.48 (s, 1H), 3.86 (s, 3H), 3.85 (s, 3H), 3.83 (s, 3H), 1.27 (s, 9H) ppm. **^{13}C NMR** (101 MHz, $CDCl_3$): δ = 154.0, 149.2, 148.7, 144.0, 128.3, 126.3, 125.9, 124.0, 120.4, 120.1, 111.3, 111.0, 110.7, 56.0, 56.0, 55.8, 36.2, 34.3, 31.6 ppm. **HR-MS** (ESI): *m/z* calculated for $C_{21}H_{26}NO_3$ $[M+H]^+$: 340.1907, found: 340.1906. **GC:** 15.50 min (method "hart"). **GCMS:** 16.94 min (method "hart"), *m/z* = 339. **R_f:** 0.25 (cyclohexane:EtOAc, 5:1).

[2] Two signals are missing: the *C*-1 carbon of the dimethoxyphenyl and the residual signal of *C*F_3 could not been resolved.

4-(Cyano-(5-dimethylethyl-4-methoxy-3-methylphenyl)methyl)1,2-dimethoxybenzene (4c)

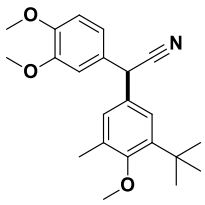

3,4-Dimethoxyphenyl acetonitrile (177 mg, 1.0 mmol) and 2-tert butyl-5-methyl anisole (357 mg, 2.0 mmol, 2.0 eq.) in 5 mL HFIP was treated with 288 C (3.0 F) with stirring. The reaction mixture was purified by silica flash column chromatography (16% → 25% EtOAc in cyclohexane) and by high pressure liquid chromatography (60% → 0% H_2O in MeCN in 90 min) to obtain the product as colorless oil (43 mg, 0.12 mmol, 12%).
^{1}H NMR (400 MHz, CD_3CN): δ = 7.20 (d, ^4J = 2.5 Hz, 1H), 7.09 (dt, $^{4,5}J$ = 2.4, 0.7 Hz, 1H), 6.93 (s, 3H), 5.20 (s, 1H), 3.78 (s, 6H), 3.73 (s, 3H), 2.28 (d, ^5J = 0.7 Hz, 3H), 1.35 (s, 9H) ppm. **^{13}C NMR** (101 MHz, CD_3CN): δ = 159.1, 150.5, 150.0, 144.1, 133.4, 132.4, 130.3, 129.7, 125.1, 121.4, 120.6, 113.0, 112.1, 61.3, 56.5, 56.4, 42.0, 35.8, 31.1, 17.5 ppm. **HR-MS** (ESI): *m/z* calculated for $C_{22}H_{27}NO_3Na$ $[M+Na]^+$: 376.1883, found: 376.1886. **GC:** 16.00 min (method "hart"). **GCMS:** 17.48 min (method "hart"), *m/z* = 353. **R_f:** 0.30 (cyclohexane:EtOAc, 5:1).

4-(Cyano-(5-bromo-4-methoxyphenyl)methyl)1,2-dimethoxybenzene (4d)

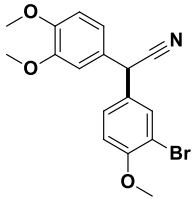

3,4-Dimethoxyphenyl acetonitrile (177 mg, 1.0 mmol) and 2-bromo anisole (374 mg, 2.0 mmol, 2.0 eq.) in 5 mL HFIP was treated with 288 C (3.0 F) with stirring. The reaction mixture was purified by silica flash column chromatography (16% → 25% EtOAc in cyclohexane) and by reversed phase column chromatography (50% → 0% H_2O in MeCN) to obtain the product as yellow oil (117 mg, 0.32 mmol, 32%). Recrystallization from MeOH yielded colorless dices.
^{1}H NMR (400 MHz, CD_3CN): δ = 7.54 (dd, $^{4,5}J$ = 2.3, 0.6 Hz, 1H), 7.36 (ddd, $^{3,4,5}J$ = 8.6, 2.4, 0.6 Hz, 1H), 7.03 (d, ^3J = 8.6 Hz, 1H), 6.96-6.88 (m, 3H), 5.24 (s, 1H), 3.86 (s, 3H), 3.79 (s, 3H), 3.77 (s, 3H) ppm. **^{13}C NMR** (101 MHz, CD_3CN): δ = 156.6, 150.6, 150.1, 133.0, 131.4, 129.6, 128.9, 120.9, 120.7, 113.7, 112.9, 112.3, 112.1, 57.0, 56.5, 56.4, 41.1 ppm. **HR-MS** (APCI): *m/z* calculated for $C_{17}H_{16}{}^{79}BrNO_3$ $[M]^+$: 361.0314, found: 361.0294, and calculated for $C_{17}H_{16}{}^{81}BrNO_3$ $[M]^+$: 363.0293, found: 363.0275. **GC:** 16.38 min (method "hart"). **GCMS:** 17.91 min (method "hart"), *m/z* = 361 (100), 363 (98). **Mp:** 68 °C. **R_f:** 0.22 (cyclohexane:EtOAc, 4:1). **CCDC-Code**: 1976461.

Author Contributions

SBB: lab work, data acquisition, writing draft; **MB**: lab work, data acquisition; **LS**: lab work; **AS**: lab work; **TM**: lab work; **DS**: x-ray single crystal analysis; **AB**: laser surface structuring; **MH**: ICP-OES analysis; **UK**: supervision ICP-OES; **WS**: supervision laser surface structuring; **SRW**: project administration, writing draft.

References

[1] Gütz, C.; Klöckner, B.; Waldvogel, S. R., *Org. Process Res. Dev.* **2016**, *20*, 26–32.

[2] Beil, S. B.; Müller, T.; Sillart, S. B.; Franzmann, P.; Bomm, A.; Holtkamp, M.; Karst, U.; Schade, W.; Waldvogel, S. R., *Angew. Chem. Int. Ed.* **2018**, *57*, 2450–2454.

[3] Rathore, R.; Bosch, E.; Kochi, J. K., *Tetrahedron* **1994**, *50*, 6727–6758.

[4] a) Goto, H.; Furusho, Y.; Miwa, K.; Yashima, E., *J. Am. Chem. Soc.* **2009**, *131*, 4710–4719; b) Shi, C.; Miao, Q.; Ma, L.; Lu, T.; Yang, D.; Chen, J.; Li, Z., *ChemistrySelect* **2019**, *4*, 6043–6047.

NMR spectra

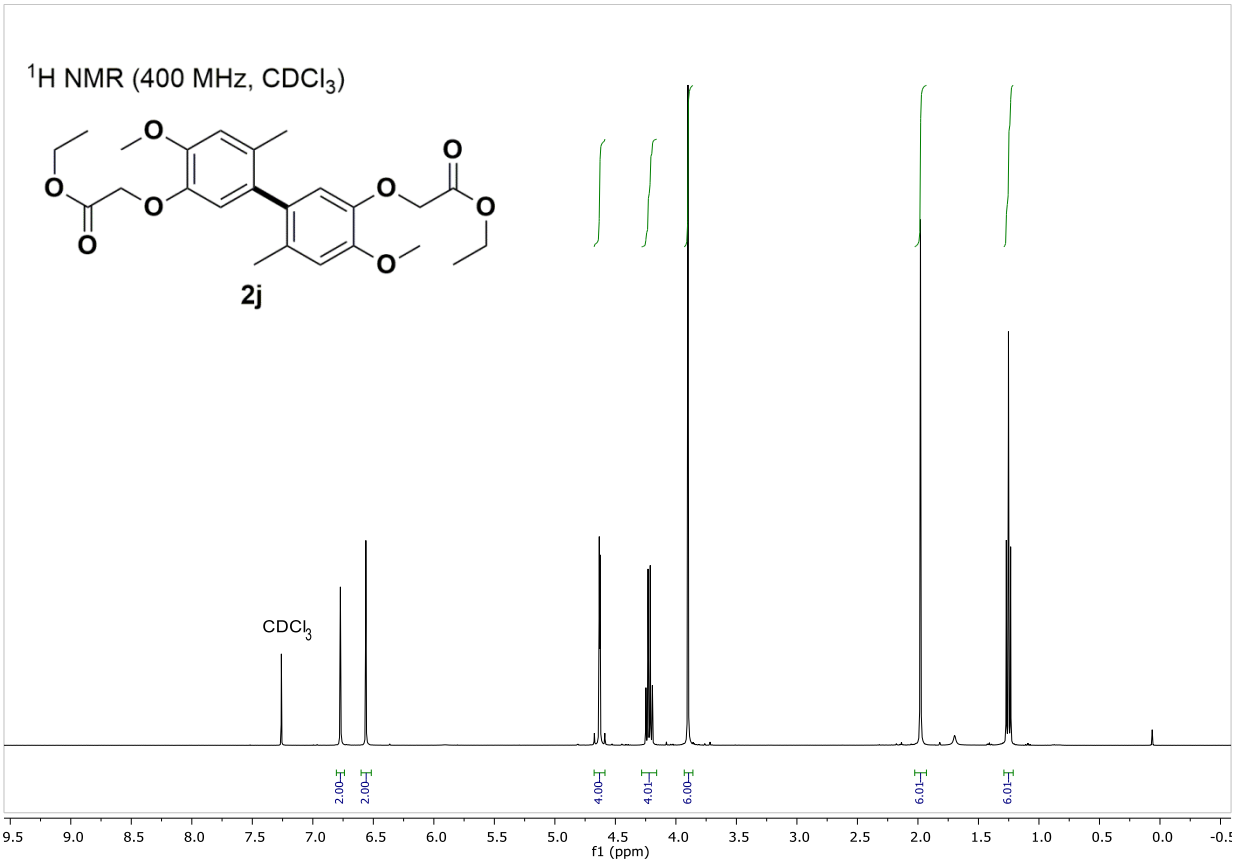
^{1}H NMR (400 MHz, $CDCl_3$)
2j
$CDCl_3$
2.00
2.00
4.00
4.01
6.00
6.01
6.01
9.5 9.0 8.5 8.0 7.5 7.0 6.5 6.0 5.5 5.0 4.5 4.0 3.5 3.0 2.5 2.0 1.5 1.0 0.5 0.0
f1 (ppm)

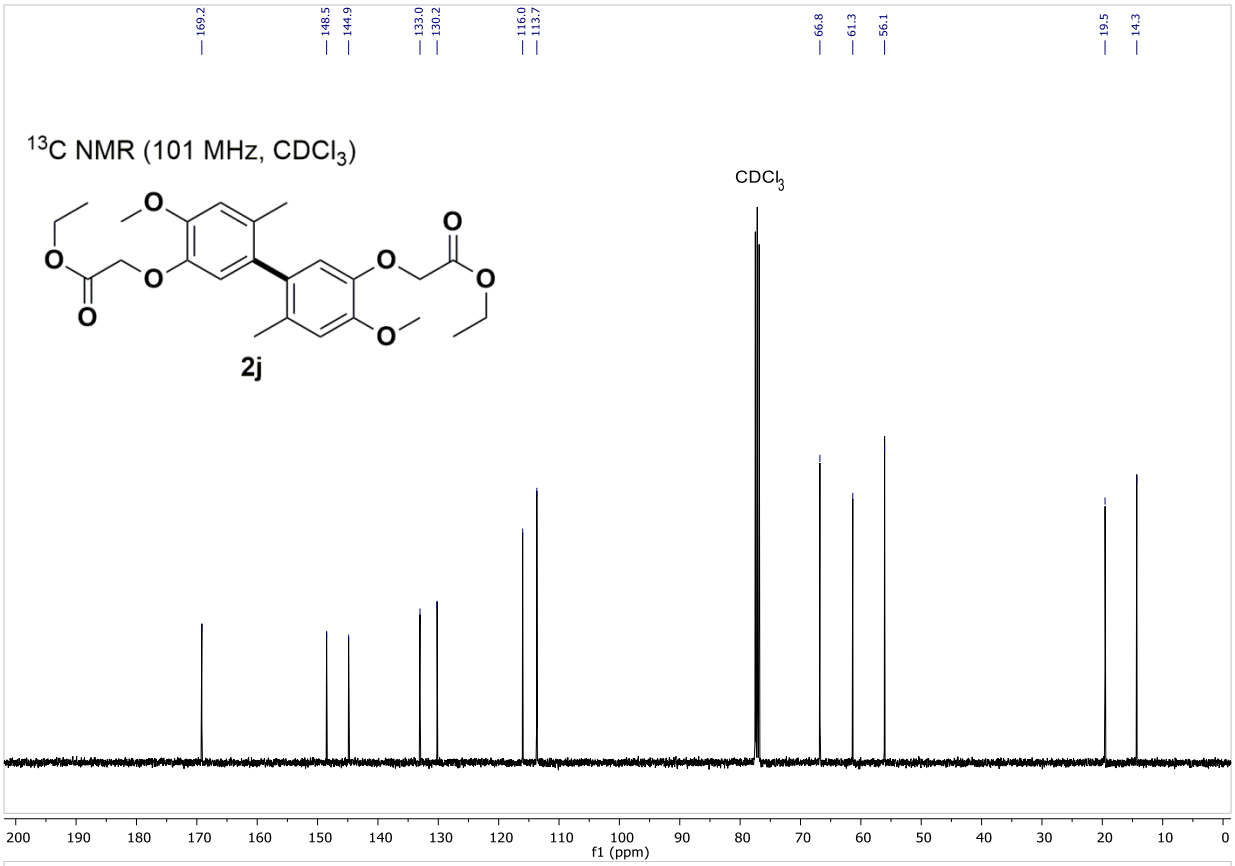
169.2
148.5
144.9
133.0
130.2
116.0
113.7
66.8
61.3
56.1
19.5
14.3
13C NMR (101 MHz, CDCl3)
CDCl3
2j
f1 (ppm)

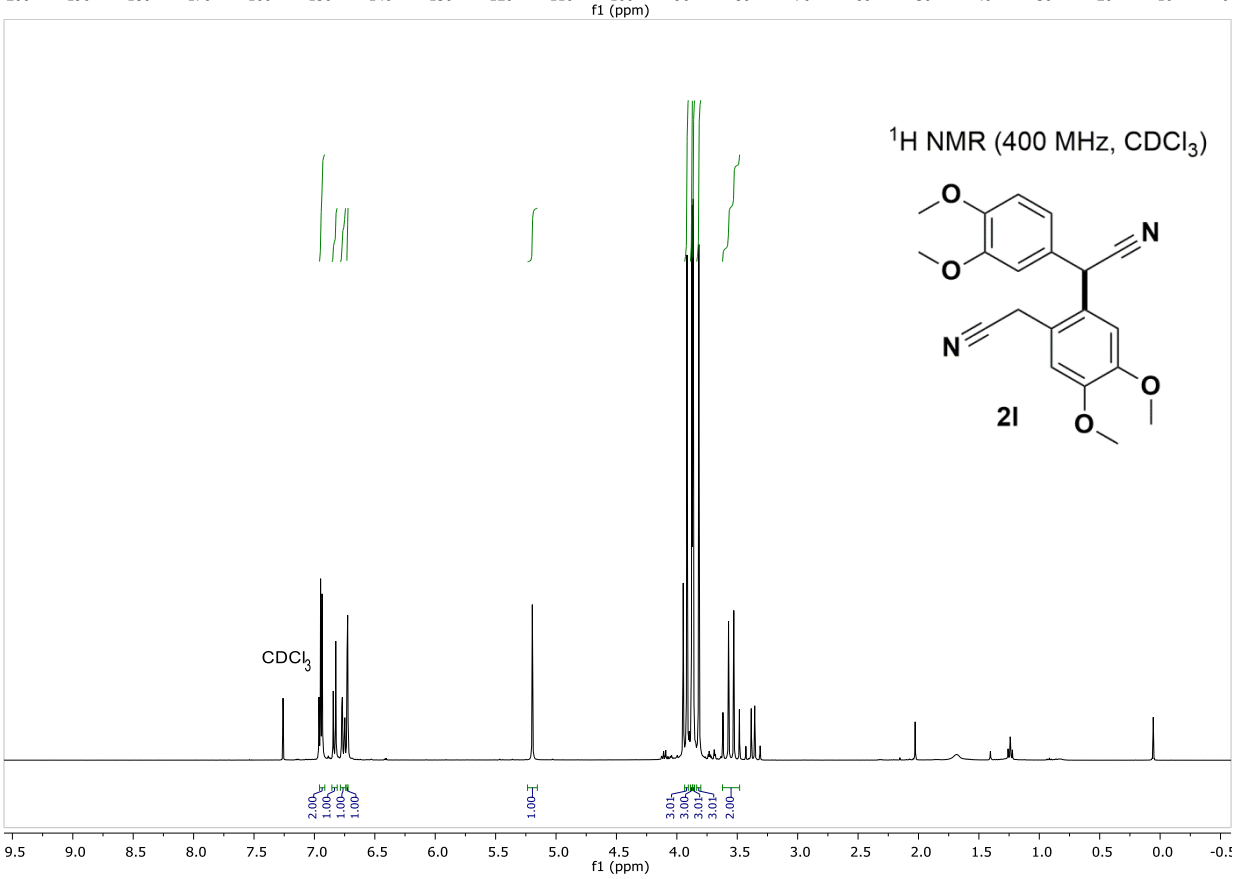
1H NMR (400 MHz, CDCl3)
CDCl3
2l
2.00
1.00
1.00
1.00
1.00
3.01
3.00
3.01
3.01
2.00
f1 (ppm)

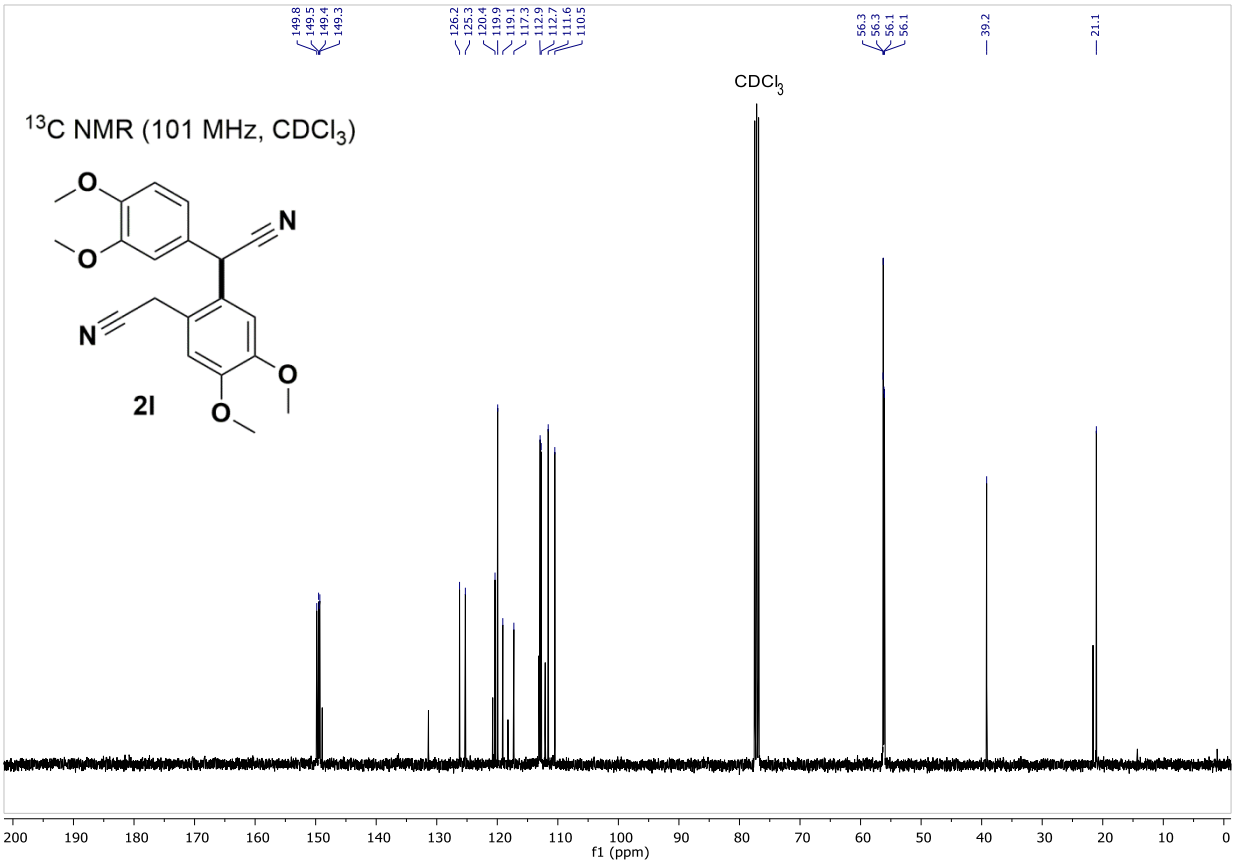
149.8
149.5
149.4
149.3
126.2
125.3
120.4
119.9
119.1
117.3
112.9
112.7
111.6
110.5
56.3
56.3
56.1
56.1
39.2
21.1
CDCl3
13C NMR (101 MHz, CDCl3)
O
O
N
N
O
O
2l
200 190 180 170 160 150 140 130 120 110 100 90 80 70 60 50 40 30 20 10 0
f1 (ppm)

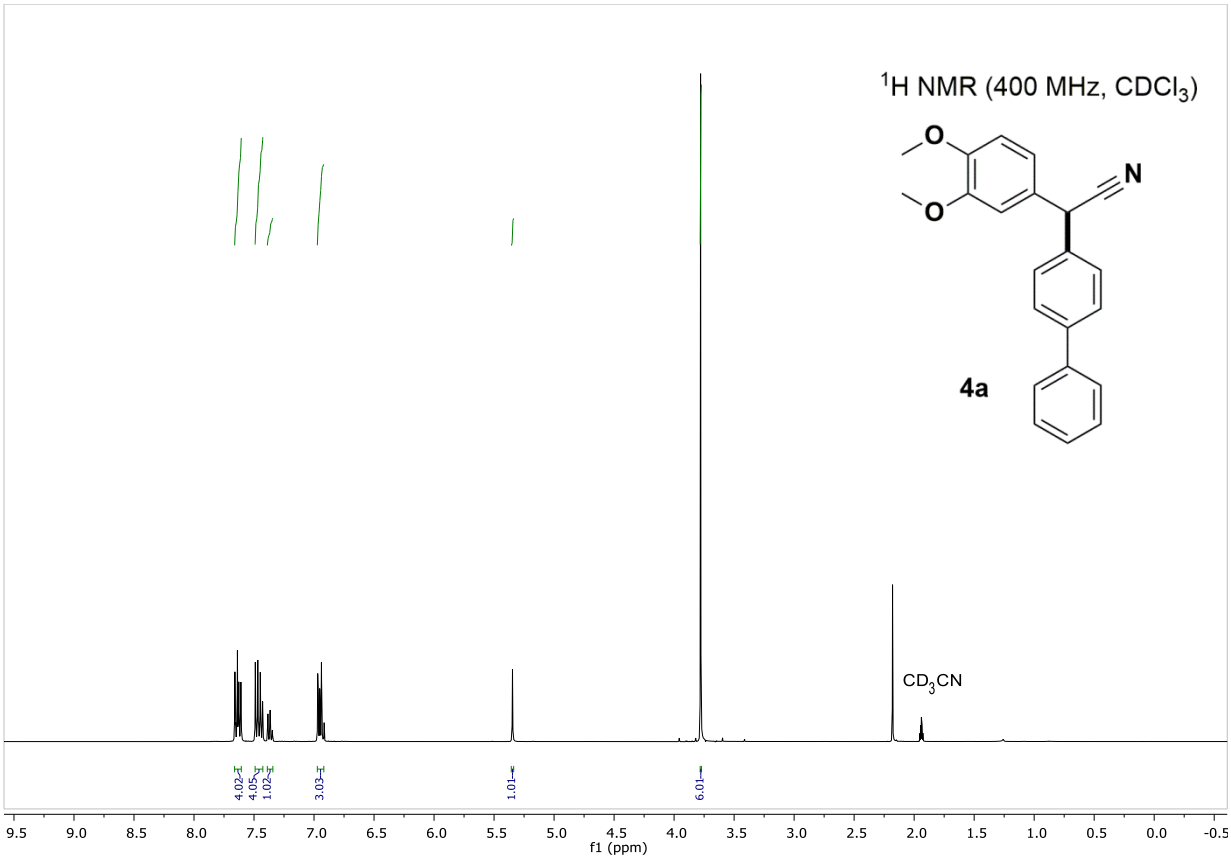
1H NMR (400 MHz, CDCl3)
O
O
N
4a
CD3CN
4.02
4.05
1.02
3.03
1.01
6.01
9.5 9.0 8.5 8.0 7.5 7.0 6.5 6.0 5.5 5.0 4.5 4.0 3.5 3.0 2.5 2.0 1.5 1.0 0.5 0.0 -0.5
f1 (ppm)

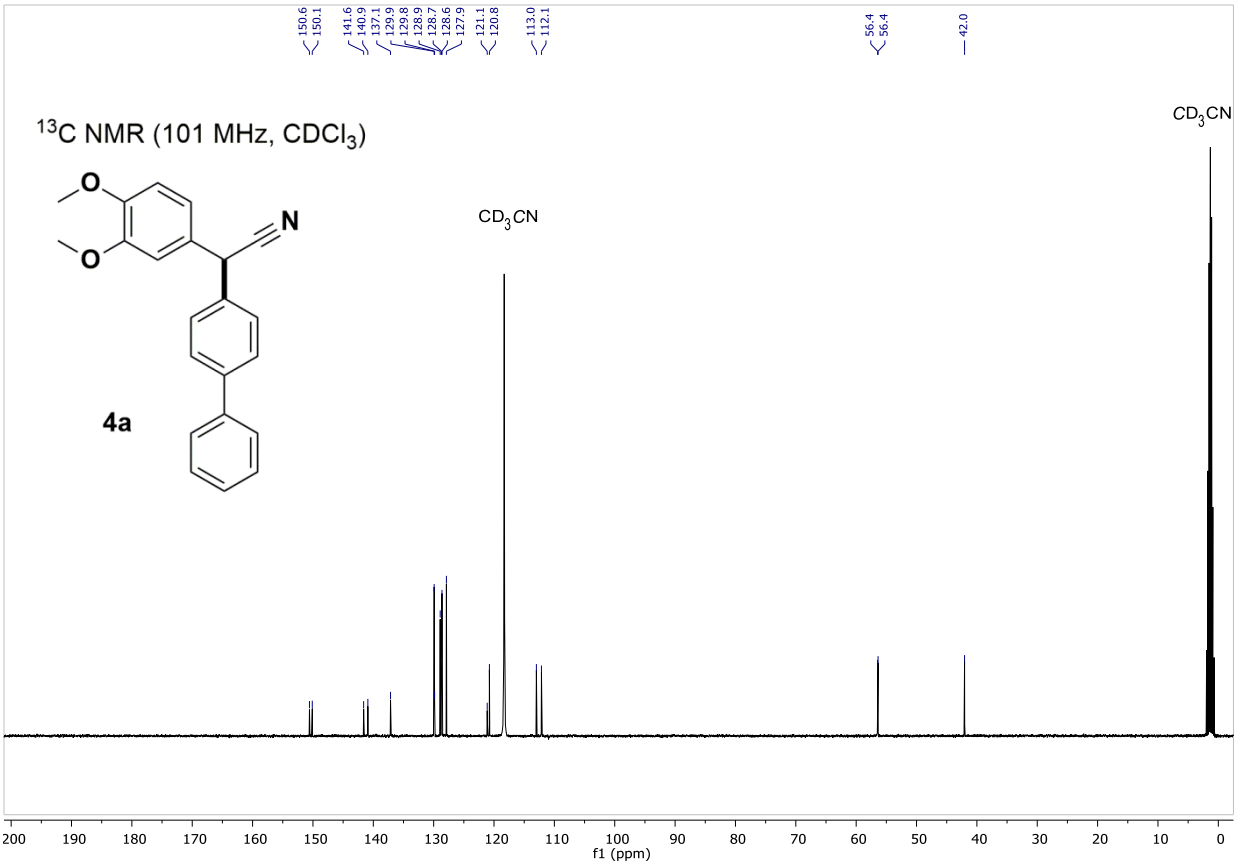
150.6
150.1
141.6
140.9
137.1
129.9
129.8
128.9
128.7
128.6
127.9
121.1
120.8
113.0
112.1
56.4
56.4
42.0
13C NMR (101 MHz, CDCl3)
CD3CN
CD3CN
O
O
N
4a
200 190 180 170 160 150 140 130 120 110 100 90 80 70 60 50 40 30 20 10 0
f1 (ppm)

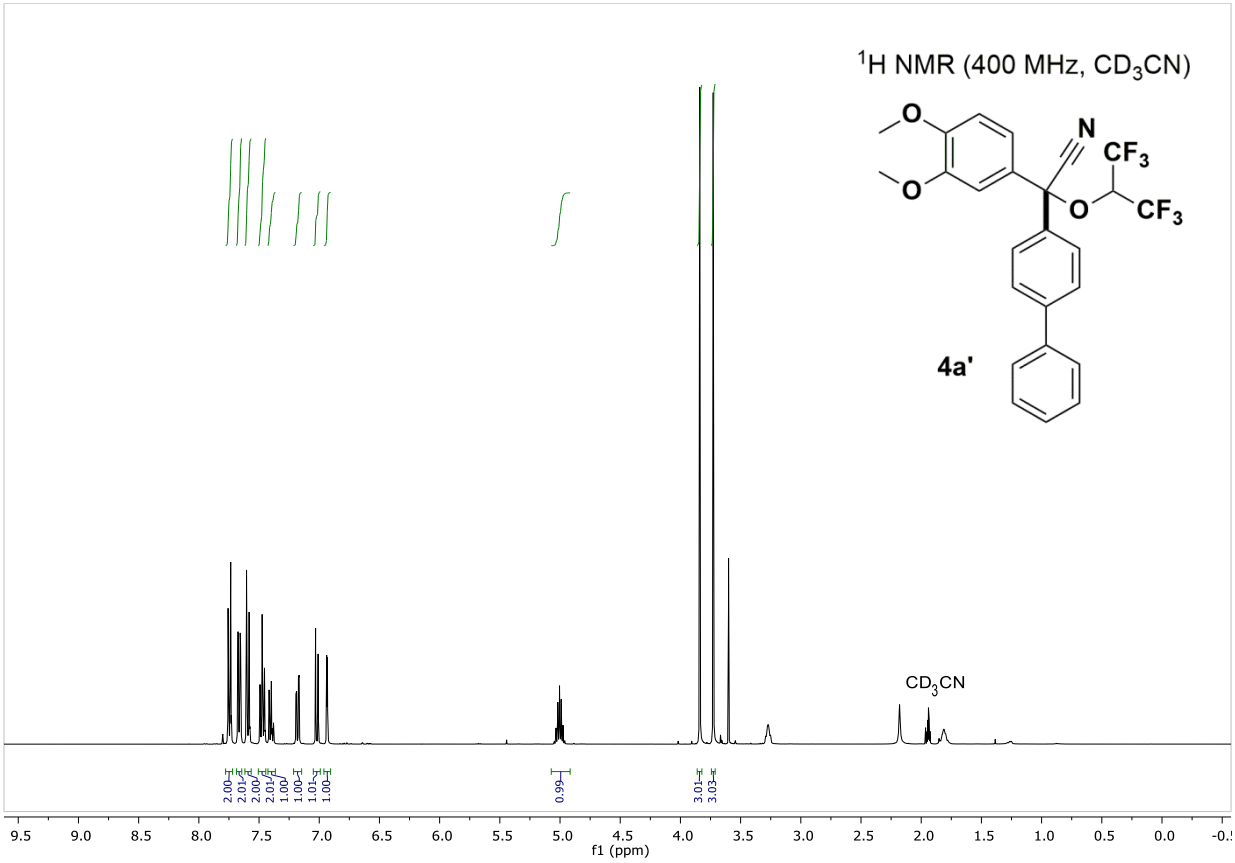
1H NMR (400 MHz, CD3CN)
O
O
N
CF3
O
CF3
4a'
CD3CN
2.00
2.01
2.00
2.01
1.00
1.00
1.01
1.00
0.99
3.01
3.03
9.5 9.0 8.5 8.0 7.5 7.0 6.5 6.0 5.5 5.0 4.5 4.0 3.5 3.0 2.5 2.0 1.5 1.0 0.5 0.0
f1 (ppm)

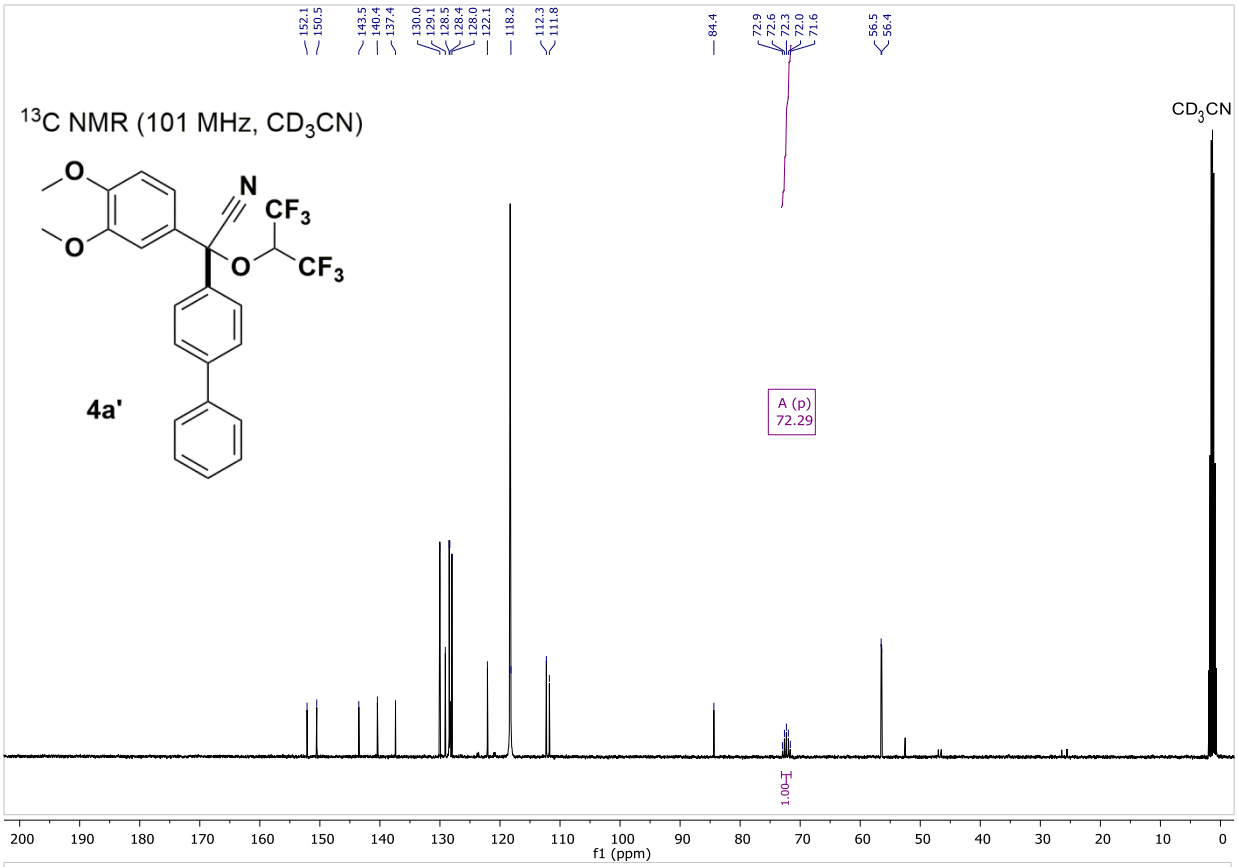
152.1
150.5
143.5
140.4
137.4
130.0
129.1
128.5
128.4
128.0
122.1
118.2
112.3
111.8
84.4
72.9
72.6
72.3
72.0
71.6
56.5
56.4
13C NMR (101 MHz, CD3CN)
CD3CN
O
O
N
CF3
O
CF3
4a'
A (p)
72.29
1.00
200 190 180 170 160 150 140 130 120 110 100 90 80 70 60 50 40 30 20 10 0
f1 (ppm)

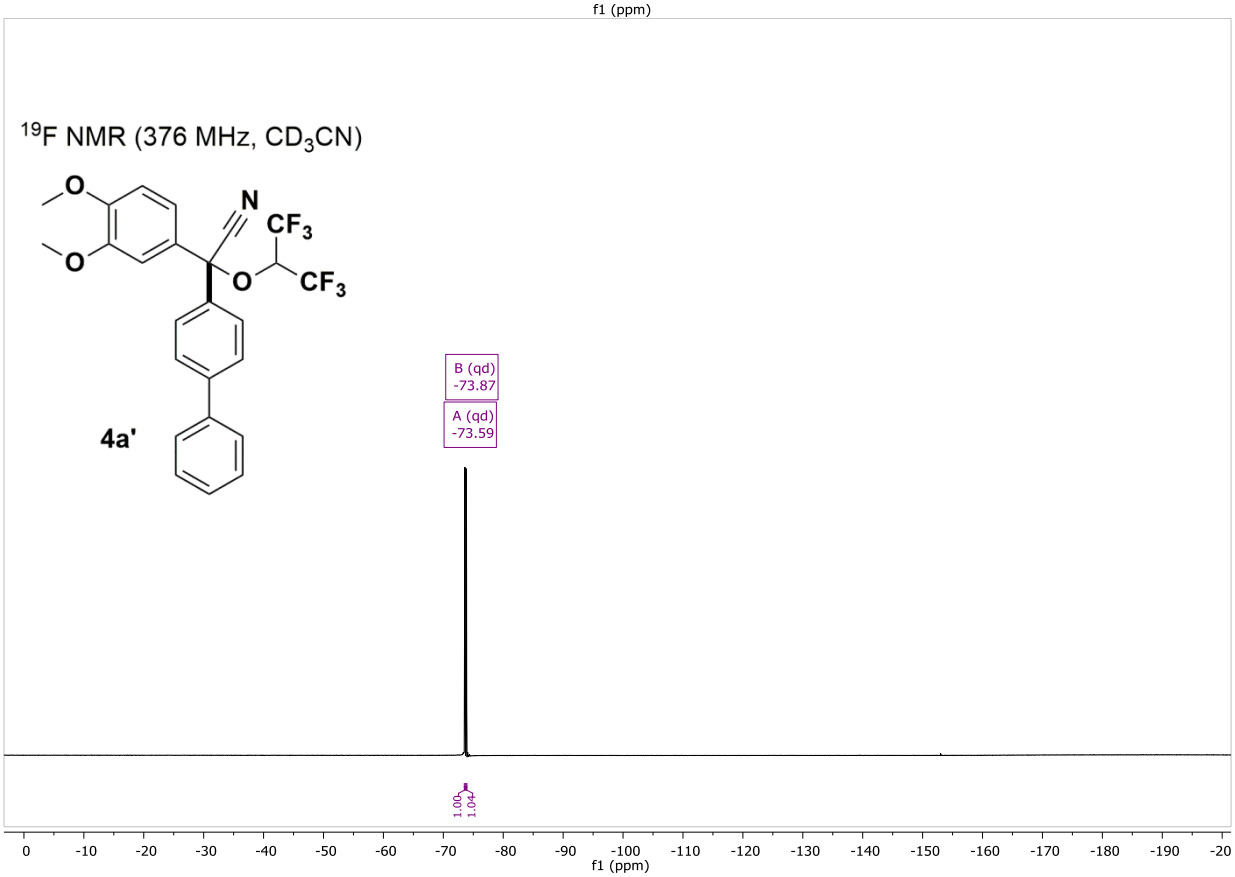
19F NMR (376 MHz, CD3CN)
O
O
N
CF3
O
CF3
4a'
B (qd)
-73.87
A (qd)
-73.59
1.00
1.04
0 -10 -20 -30 -40 -50 -60 -70 -80 -90 -100 -110 -120 -130 -140 -150 -160 -170 -180 -190 -20
f1 (ppm)

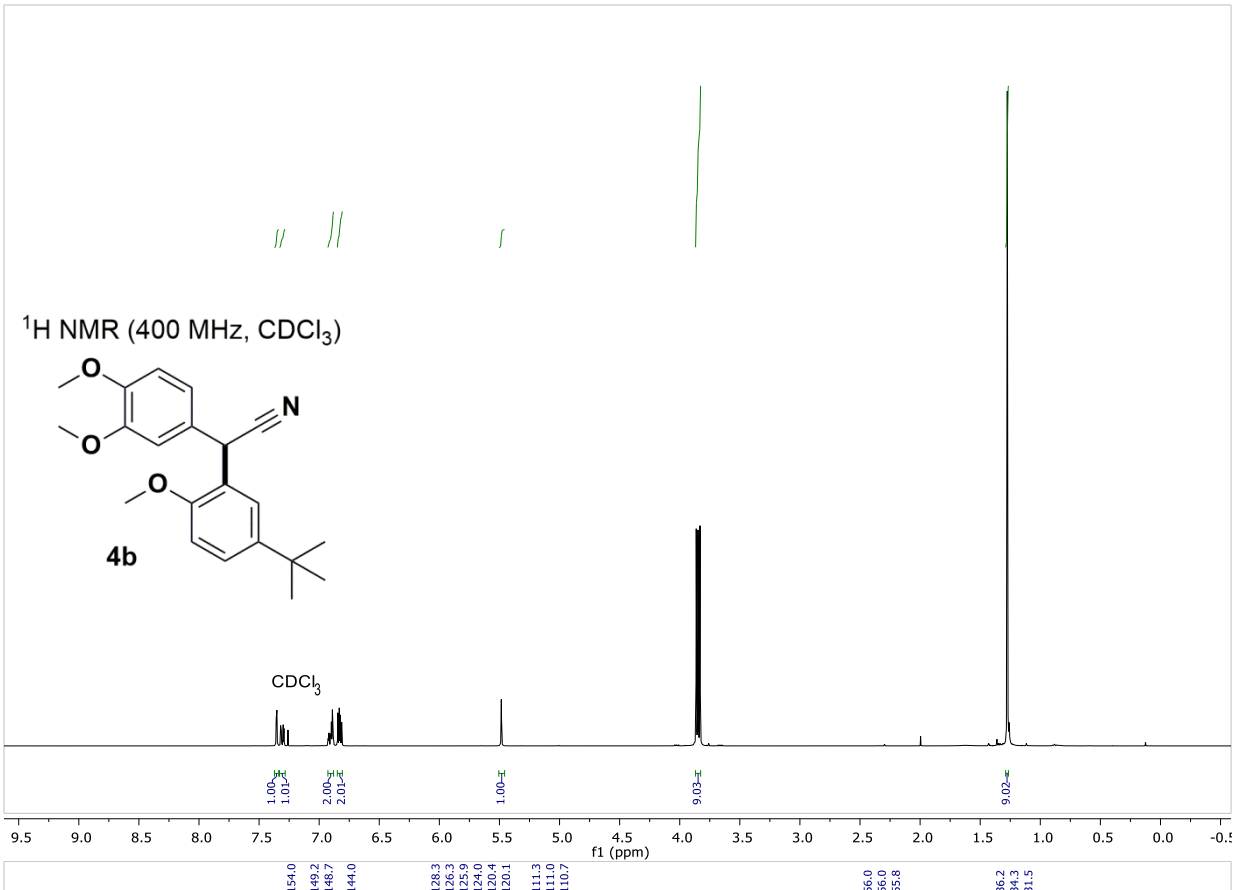
^{1}H NMR (400 MHz, $CDCl_3$)
O
O
O
N
4b
$CDCl_3$
1.00
1.01
2.00
2.01
1.00
9.03
9.02
9.5 9.0 8.5 8.0 7.5 7.0 6.5 6.0 5.5 5.0 4.5 4.0 3.5 3.0 2.5 2.0 1.5 1.0 0.5 0.0
f1 (ppm)

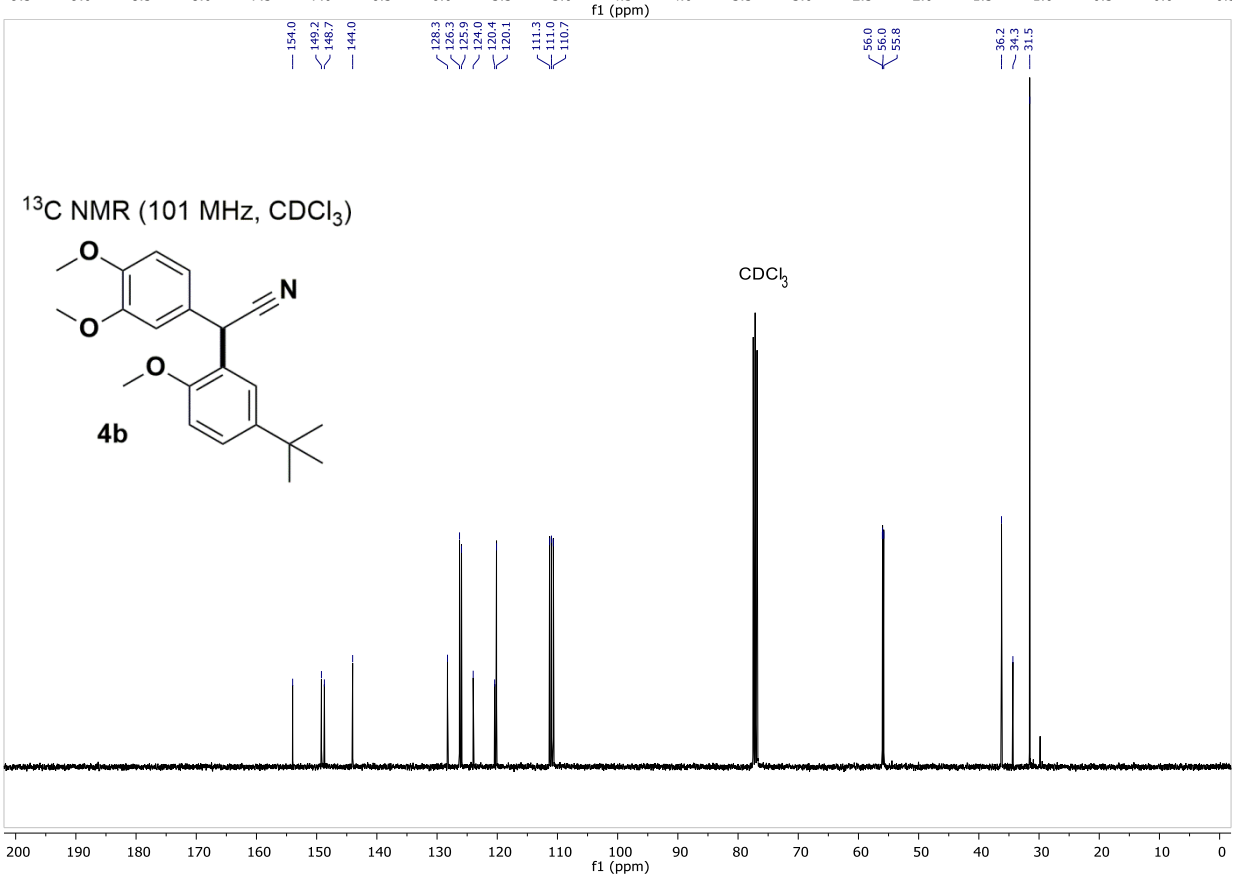
154.0
149.2
148.7
144.0
128.3
126.3
125.9
124.0
120.4
120.1
111.3
111.0
110.7
56.0
56.0
55.8
36.2
34.3
31.5
^{13}C NMR (101 MHz, $CDCl_3$)
O
O
O
N
4b
$CDCl_3$
200 190 180 170 160 150 140 130 120 110 100 90 80 70 60 50 40 30 20 10 0
f1 (ppm)

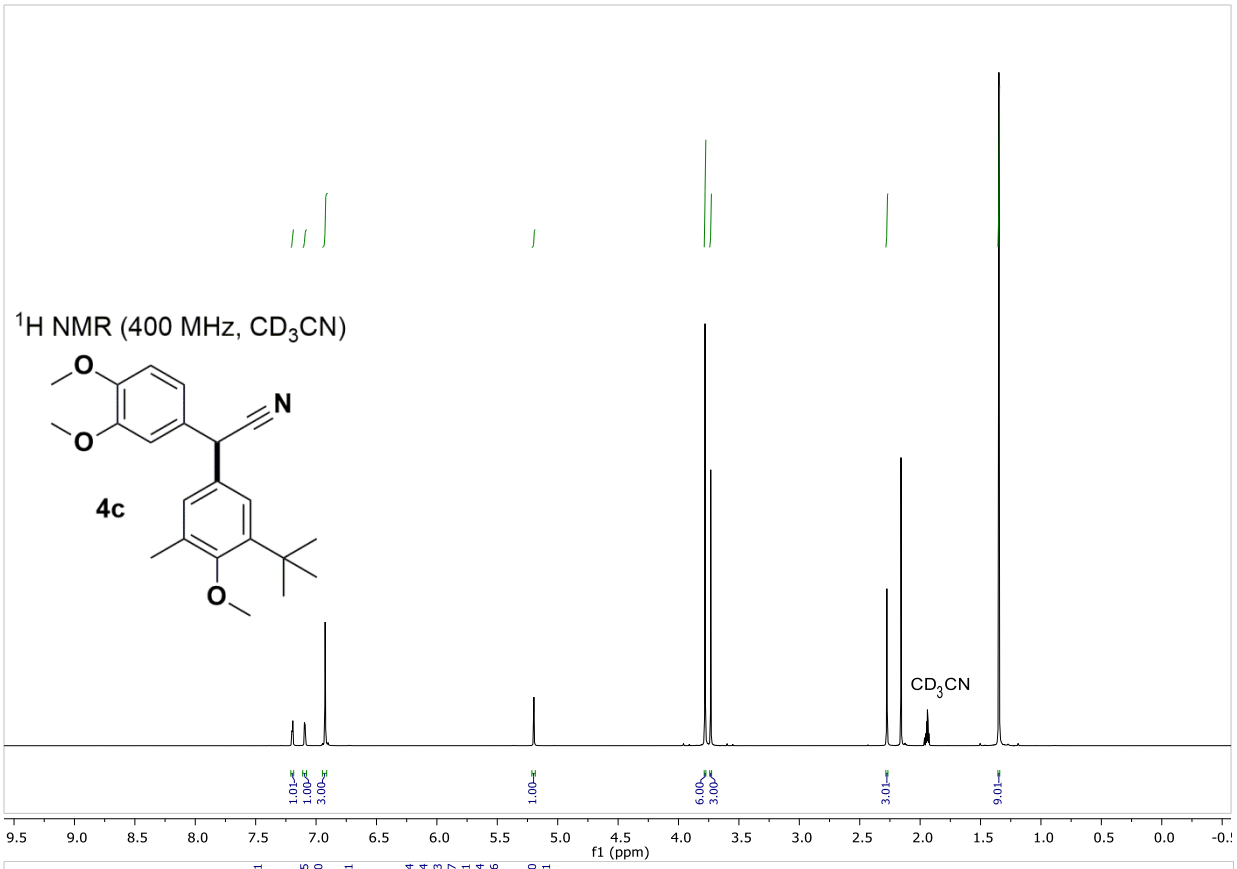
^{1}H NMR (400 MHz, CD_3CN)
4c
CD_3CN
f1 (ppm)

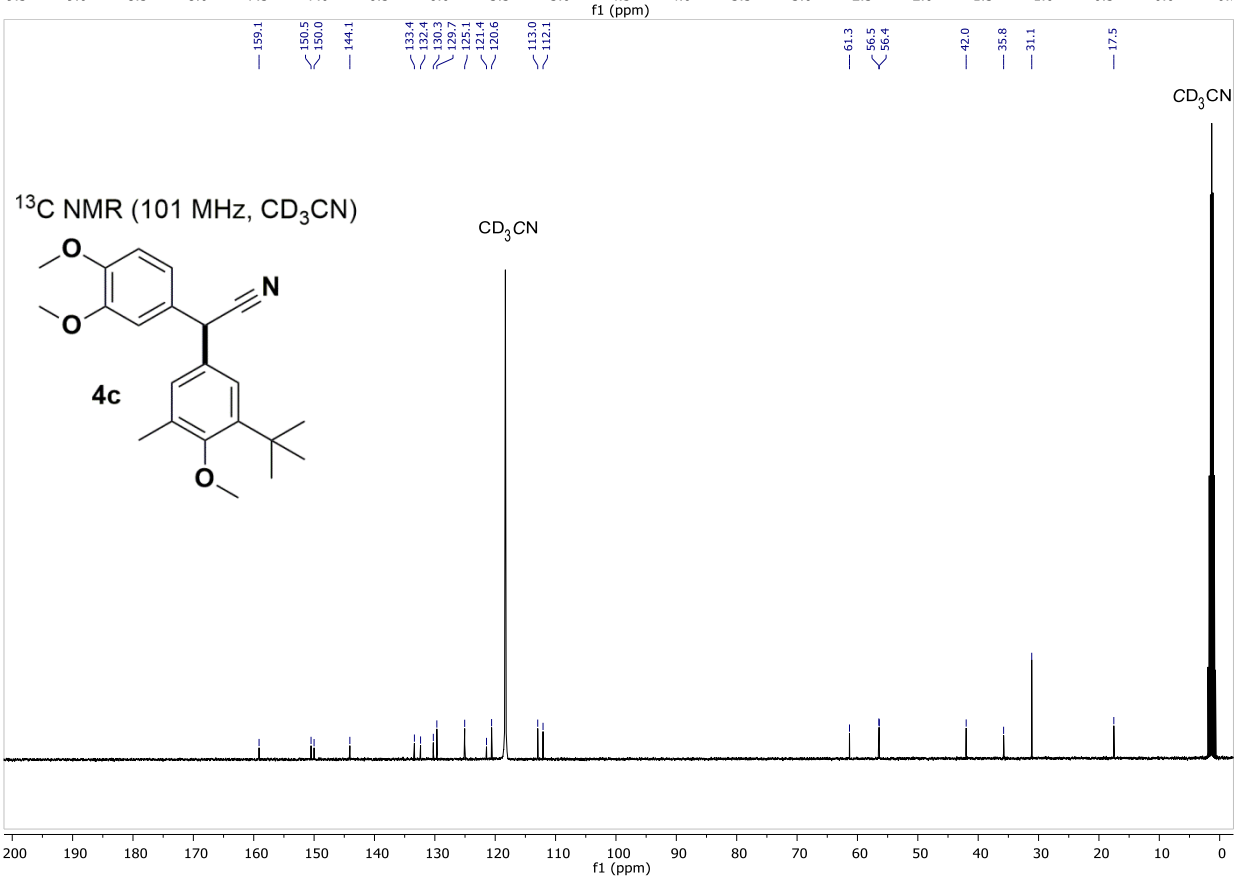
^{13}C NMR (101 MHz, CD_3CN)
4c
CD_3CN
CD_3CN
f1 (ppm)

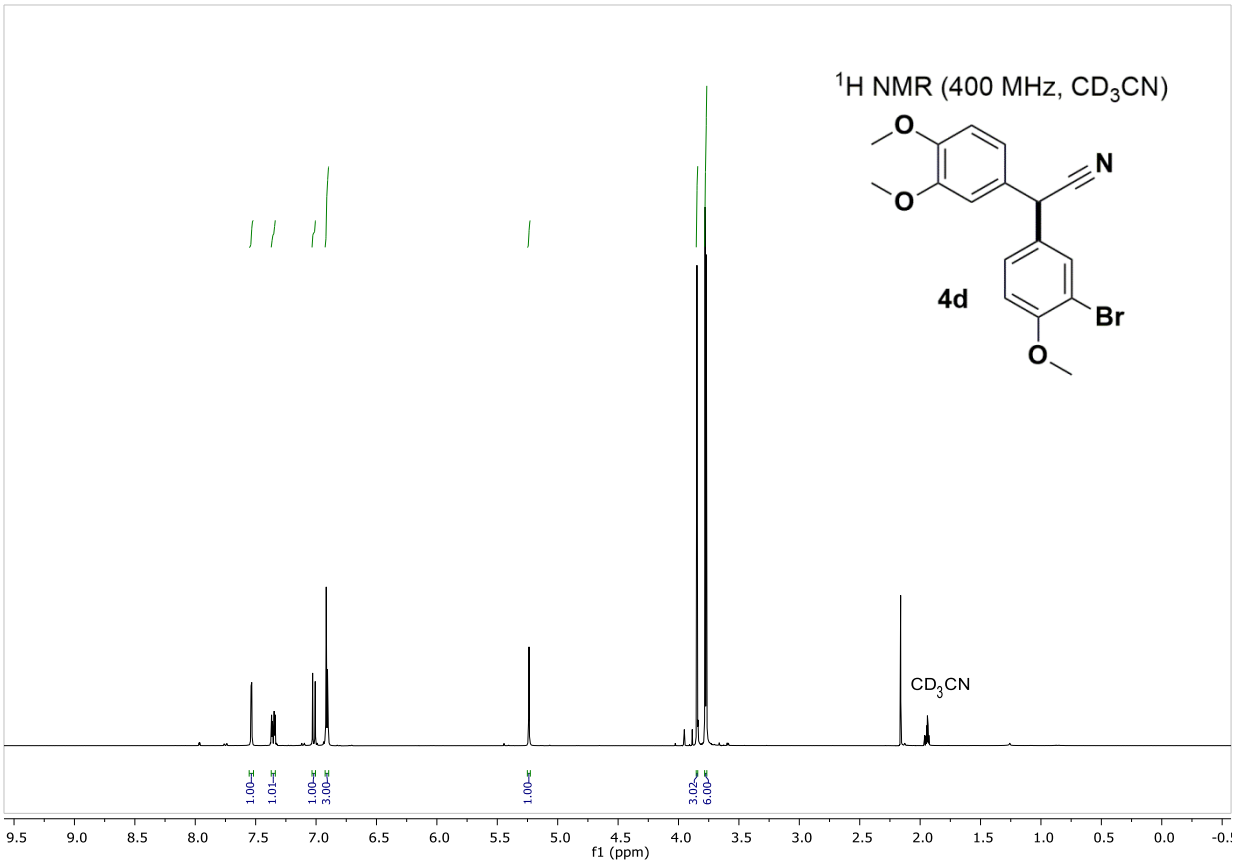
^{1}H NMR (400 MHz, CD_3CN)
4d
Br
O
N
CD_3CN
1.00
1.01
1.00
3.00
1.00
3.02
6.00
f1 (ppm)

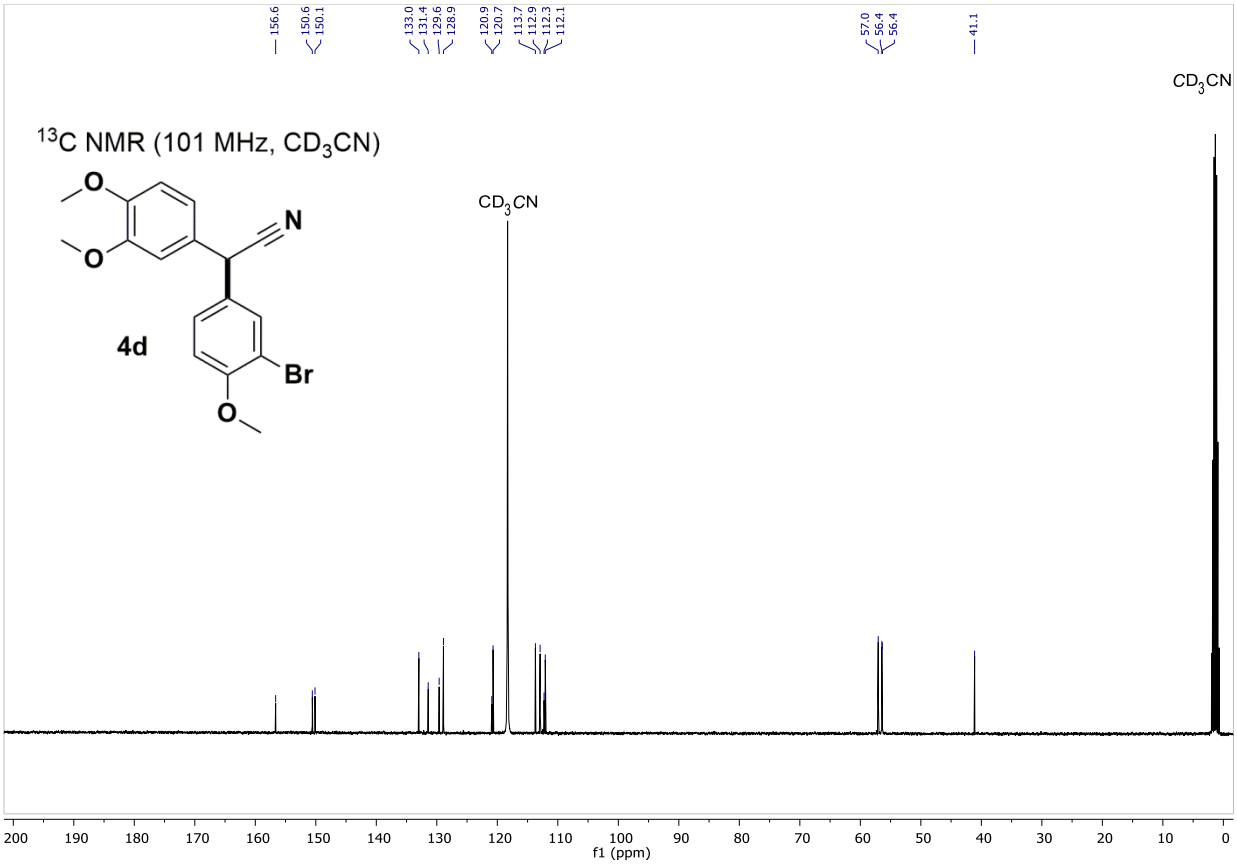
^{13}C NMR (101 MHz, CD_3CN)
4d
Br
O
N
CD_3CN
156.6
150.6
150.1
133.0
131.4
129.6
128.9
120.9
120.7
113.7
112.9
112.3
112.1
57.0
56.4
56.4
41.1
f1 (ppm)